Journal of
Nanoscience and Nanotechnology
Vol. 10, 1563–1583, 2010

A Review on Inorganic Nanostructure Self-Assembly

Yuehui Wang[1,2,*] and Weidong Zhou[1]

[1] Department of Electrical Engineering, NanoFAB Center, University of Texas at Arlington, Arlington, TX 76019-0072, USA
[2] Department of Chemistry and Biology, University of Electronic Science and Technology of China, Zhongshan Institute, Zhongshan 528402, China

In recent years, there has been a growing interest in the self-assembly process for the fabrication of micro- and nano-scale structures for various device applications. The success of these applications requires the development of a versatile assembly process for producing large area ordered arrays. In this article, we review recent advances, particularly related to photonic material and device applications, based on self-assembly processes, with the focus on the processes for inorganic structure self assembly. We first discuss major forces guiding the particle self-assembly in the wet coating technology. Then we review device applications and recent advances based on three kinds of wet coating technologies, including dip coating, spin coating and convective coating. Finally, a conclusion will be given, with discussions given on future perspectives.

Keywords: Self-Assembly, Wet Coating, Forces, Dip Coating, Spin Coating, Convective Coating.

REVIEW

CONTENTS

1. INTRODUCTION

Nanotechnology is an art of manipulating materials at the atomic scale. This deals with the design and manufacturing of very small features in the range of nanometer scales. Most nanophotonic devices are fabricated based on the lithographic top-down approaches, with optical or electron-beam lithography, for the desired controllability and integration requirements. In recent years, there has also been a growing interest in bottom-up self-assembly processes for the fabrication of micro- and nano-scale structures for applications in photonic materials,[1,2] optoelectronic devices,[3–5] chemical and biochemical sensors,[6,7] template processing,[8,9] etc. The basic building blocks are usually micro-, submicro- and nano-particles of metal, semiconductor, macromolecule, dielectric, and magnetic materials, etc.[10,11] These particles have fascinating optical and electronic properties[12–14] due to the special assembly geometry. For example, the colloidal crystals with the precise ordering of particles can control the propagation of photons as photonic manipulator, or photonic crystals.[15] Ordered monolayers of particles were applied as convenient micro-patterned surfaces for studying the cell adhesion.[16] In addition, cooperative effects emerge when nanoparticles are arranged as the ordered arrays in two-dimensional (2D), or three-dimensional (3D) superlattice structures.[17–21] It is thus very important to investigate the collective properties of micro- and nanoscale structures for device applications.[3,22,23]

Self-assembly is a spontaneous formation of structures due to the chemical interactions between the particles.[24–26] As the size of the system reduces, capillary forces dominate over a few other forces like gravitational, hydrodynamic, magnetic, electrostatic and surface adhesion.[27,28] It is the selective control of the non-covalent interactions which creates structured components at molecular levels. Self-assembly is governed by the interaction between nanoparticles which includes capillarity and wetting ability of the substrate. Many different types of self-assembly processes have been proposed, such as

*Author to whom correspondence should be addressed.

1533-4880/2010/10/1563/021 doi:10.1166/jnn.2010.2030

Journal of
Nanoscience and Nanotechnology
Vol. 10, 1–21, 2010

A Review on Inorganic Nanostructure Self-Assembly

Yuehui Wang[1, 2, *] and Weidong Zhou[1]

[1] *Department of Electrical Engineering, NanoFAB Center, University of Texas at Arlington, Arlington, TX 76019-0072, USA*
[2] *Department of Chemistry and Biology, University of Electronic Science and Technology of China, Zhongshan Institute, Zhongshan 528402, China*

In recent years, there has been a growing interest in the self-assembly process for the fabrication of micro- and nano-scale structures for various device applications. The success of these applications requires the development of a versatile assembly process for producing large area ordered arrays. In this article, we review recent advances, particularly related to photonic material and device applications, based on self-assembly processes, with the focus on the processes for inorganic structure self assembly. We first discuss major forces guiding the particle self-assembly in the wet coating technology. Then we review device applications and recent advances based on three kinds of wet coating technologies, including dip coating, spin coating and convective coating. Finally, a conclusion will be given, with discussions given on future perspectives.

Keywords: Self-Assembly, Wet Coating, Forces, Dip Coating, Spin Coating, Convective Coating.

REVIEW

CONTENTS

1. INTRODUCTION

Nanotechnology is an art of manipulating materials at the atomic scale. This deals with the design and manufacturing of very small features in the range of nanometer scales. Most nanophotonic devices are fabricated based on the lithographic top-down approaches, with optical or electron-beam lithography, for the desired controllability and integration requirements. In recent years, there has also been a growing interest in bottom-up self-assembly processes for the fabrication of micro- and nano-scale structures for applications in photonic materials,[1, 2] optoelectronic devices,[3–5] chemical and biochemical sensors,[6, 7] template processing,[8, 9] etc. The basic building blocks are usually micro-, submicro- and nano-particles of metal, semiconductor, macromolecule, dielectric, and magnetic materials, etc.[10, 11] These particles have fascinating optical and electronic properties[12–14] due to the special assembly geometry. For example, the colloidal crystals with the precise ordering of particles can control the propagation of photons as photonic manipulator, or photonic crystals.[15] Ordered monolayers of particles were applied as convenient micro-patterned surfaces for studying the cell adhesion.[16] In addition, cooperative effects emerge when nanoparticles are arranged as the ordered arrays in two-dimensional (2D), or three-dimensional (3D) superlattice structures.[17–21] It is thus very important to investigate the collective properties of micro- and nanoscale structures for device applications.[3, 22, 23]

Self-assembly is a spontaneous formation of structures due to the chemical interactions between the particles.[24–26] As the size of the system reduces, capillary forces dominate over a few other forces like gravitational, hydrodynamic, magnetic, electrostatic and surface adhesion.[27, 28] It is the selective control of the non-covalent interactions which creates structured components at molecular levels. Self-assembly is governed by the interaction between nanoparticles which includes capillarity and wetting ability of the substrate. Many different types of self-assembly processes have been proposed, such as

*Author to whom correspondence should be addressed.

physical, chemical, Layer-by-Layer (LbL), molecular, and evaporation-induced self assemblies.[26, 29–33]

Shown in Figure 1 are examples of four major types of self-assembled structures. Monolayer and multilayers structures are often found applications in optical coating and photonic crystal structures. Patterned assembly, i.e., a combination of top-down and bottom-up approaches, where self assembly occurs in precisely defined pattern regions, are more attractive for device integration. Finally, self assembly in liquid often finds applications in liquid crystals and biosensor applications.

The wet assembly process has been proven to be an extremely powerful and versatile pathway to produce micro- and nanoscale structures at a high process rate. The wet assembly process includes the assembly of structures from particles dispersed in colloids or suspension, the assembly of structures on technologically relevant substrates or surface of liquids, or the assembly of self-assembled arrays into structures suitable for practical applications.

The wet assembly process has the following inherent advantages: (1) low temperature processing, (2) highly controllable coating thickness, (3) easily shaping the materials into complex geometries, (4) strong adhesion of coating to the substrate (5) compositional flexibility, (6) three-dimensional structure, (7) large-area coating, and (8) economic, convenient and experimental simplicity. However, despite its advantages, the wet assembly technique never arrives at its full industrial potential due to some limitations, e.g., weak bonding, low wear-resistance, and difficult controlling of defects. In particular, the thick coating with crack-free property is an indispensable requirement. The present wet assembly technique, especially sol–gel technique is very substrate-dependent, and the thermal expansion mismatch limits its wide application. The tremendous effort dedicated to this field during the past few decades. Significant progresses have been reported, which boosted the development of sol–gel chemistry and potential technological applications. At present, major research efforts in wet assembly technique focus on the fabrication of large-area, highly-ordered, repeatable and scalable structures with high productivity, and further design and manipulate these structures to achieve well-tailored chemical-physical characteristics for advanced applications.

The realization of particles assembly into ordered arrays focuses on two steps: (1) understanding of the interaction between particles and the main physicochemical variables governing formation of ordered 2D and 3D particles arrays; (2) understanding of assembly process characteristics for the desired structures. We tried to extract these two issues on this review. A comprehensive review on various unconventional techniques for fabricating complex nanostructures was recently published.[34–38] Here, we concentrate on the wet assembly technique, main including dip coating, spin coating and convective coating,

Dr. Yuehui Wang received a Ph.D. degree in Material Science and Engineering from South China University of Technology in 2004 and joined Tsinghua University, P. R. China as a Postdoc in Material Science and Engineering (2005). Follow this, she worked as a postdoc at the university Texas at Arlington with Professor Zhou and Profosser Tao. Her current interests involve the assembly of nano-, microparticles and the study of their characteristic optical properties and their application solar cells.

Dr. Weidong Zhou received his B.E. and M.S. degrees from Tsinghua University, China, and Ph.D. degree from University of Michigan, Ann Arbor, all in Electrical Engineering. Currently Dr. Zhou is an Associate Professor of Electrical Engineering at University of Texas at Arlington (UTA). His current research projects include photonic crystals, infrared sensors, silicon photonics and solar cells, with funding support from US National Science Foundation, US Department of Defense Agencies (AFOSR, AFRL, ARO, DARPA) and recently a multi-million MURI center project (Multidisciplinary University Research Initiative program), etc. To date, Dr. Zhou has authored or co-authored over 120 peer reviewed journal publications, conference presentations and invited talks. He serves as various proposal and journal reviewers, and various conference committees. Dr. Zhou's major awards include prestigious *Outstanding Student of Beijing City* (Beijing, 1992), *Outstanding Graduates Award* (Tsinghua Univ., Gold medal, 1993); *IEEE/LEOS Graduate Student Fellowship award* (IEEE/LEOS, 2000), *Rackham Predoctoral Fellow award* (2000–2001, Michigan), and *UTA College of Engineering Research Excellence Awards* (2007, 2008). Dr. Zhou is a senior member of IEEE, member of OSA, SPIE, MRS.

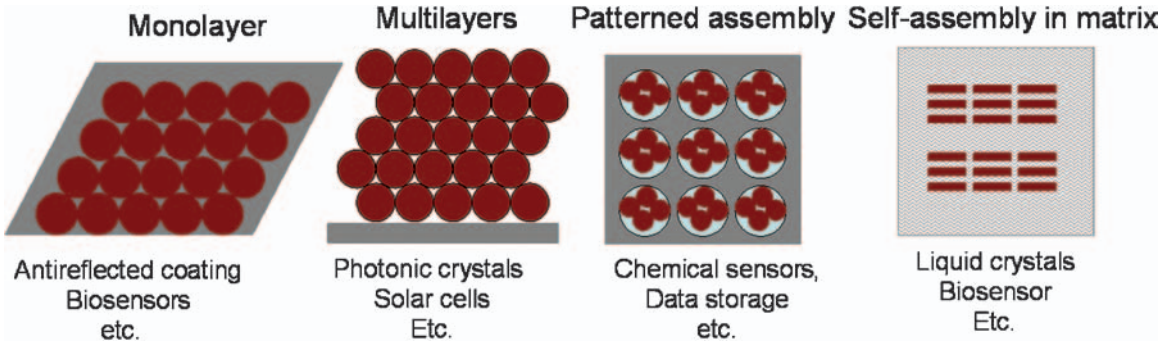

Fig. 1. Various particles self-assembly structures and their applications.

according to our results and other researcher groups. We are dedicated to the understanding of these techniques process, mechanisms and development in the field of particle self-assembly. These assembly processes are the promising techniques for practical applications because they are inexpensive, high-throughput, and suitable for 2D and 3D self-assembly structures on any types of substrates.

2. THE FORCES GUIDING THE PARTICLE SELF-ASSEMBLY PROCESS

To fabricate desired assembly structures of particles, the understanding of the assembly dynamics is of critical importance in our ability to construct these systems accurately. Assembly by wet assembly process usually takes place in solution, where the particles experience a sequence of different phases, namely suspension, migration, deposition/crystallization, and drying/fixation. Various types of interactions take place simultaneously and the resultant structure of the self-assembly is a complex balance of the attractive and repulsive interactions. The forces operating at the colloidal length scale have been well studied. Scientists and engineers presently seek to employ these forces and interactions to tailor particle self-assembly into usable architectures. Refs. [35, 39, 40] gave more comprehensive reviews, here we discuss several dominating forces which guiding particle self-assembly in the wet assembly process, such as *van der Waals* (vdW), electrostatic, depletion, hydrophobic forces, capillary force and viscous drag force, etc.

2.1. DLVO Theory and Non-DLVO Theory

The interaction and behavior of surfaces or colloids are quantitatively described by DLVO (*Derjaguin-Landau-Verwey-Overbeek*) theory and the non-DLVO interactions.[41] The DLVO theory is a classical model of colloid stability to describe the force between charged surfaces interacting through a liquid medium and combines the effects of the vdW attraction and the electrostatic repulsion.

Owing to the assumptions used that the intervening liquid has a uniform density and orientation profile for the vdW calculation, the DLVO model fails to correctly describe interactions between two surfaces/particles closer than a few nanometers apart. It is reasonable to believe there are non-DLVO force effects. Non-DLVO force works as repulsive forces in the case of hydrophilic nanoparticles, such as silica nanoparticles, and possibly originates from the hydrogen bonding[42, 43] or gel layer.[44, 45] Non-DLVO force is usually stronger than DLVO-force when the surface distance of two nanoparticles reaches 2–3 nm. In the case of large nanoparticle solution, as particles approach to each other, DLVO force first become the dominant forces, whereas for small nanoparticles, non-DLVO force takes effect ahead of DLVO force. On the other hand, non-DLVO force is associated with water near to or absorbed on nanoparticles surfaces so that it will be weakening and eventually disappear due to the evaporation. Therefore, the ordered structure might be dwindled into small domains with similar sizes. Although nanoparticles are well ordered within these domains, defects inevitably remain at domain boundaries. Moreover, as the size of nanoparticles becomes smaller, this disordering effect becomes more dominant because the working distance of solvent-dependent forces is more comparable to the scale of smaller nanoparticles. These long-range repulsive forces or short-range solvent-dependent forces are accompanied by a low surface coverage or a disordering process, which inevitably results in the formation of domains and boundaries in the nanoparticle assembly structures.[41]

2.2. Van der Waal Forces and Electrostatics

The *van der Waal* (vdW) attraction forces are the primary cause for particle aggregation and/or adhesion to substrate surfaces. They are weak attractive forces between atoms or nonpolar molecules caused by a temporary change in dipole moment arising from a brief shift of orbital electrons to one side of one atom or molecule, creating a similar shift in adjacent atoms or molecules. Figure 2 gives

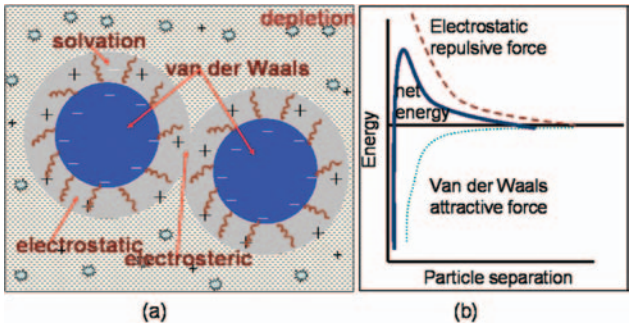

Fig. 2. (a) Typical colloidal forces between two particles. (b) The energy profile the stability of a colloidal system is determined by the sum of the electrostatic repulsive force and van de Waals attractive forces which the particles experience as they approach one another. Reprinted with permission from [35], D. Velegol, *J. Nanophoton.* 1, 012502 **(2007)**. © 2007, SPIE.

REVIEW

a typical schematic of colloidal forces between two particles (Fig. 2(a)), along with the energy profile responsible for the stability of a colloidal system (Fig. 2(b)).[35] The range of vdW forces is in the order of a nanometer or less when they act between two atoms/molecules, however these forces can cover much longer distances when colloidal particles are considered. The vdW interaction energy for the geometry described can be modeled as:[46]

$$\Delta G_{1w2}^{\mathrm{vdW}} = \frac{-A_{1w2r}}{6d}\left\{1+\frac{d}{2r+d}+\frac{d}{r}\ln\left(\frac{d}{2r+d}\right)\right\} \quad (1)$$

where A_{1w2} is unretarded Hamaker constant for a sphere of radius, r, and a flat plate suspended in water, about equal to $(A_{11}^{1/2}-A_{ww}^{1/2})(A_{22}^{1/2}-A_{ww}^{1/2})$.

They always exist between two particles and can be greatly reduced by "index matching."[47] If the relative permittivity of one particle is greater than that of the surrounding medium, while the other particle's is less, then the vdW forces in fact become repulsive.[48] The vdW forces have been tested to work well for micron-size particles,[49] while the phenomenon is less predictable for nanocolloids.[50, 51] Recently, Kim and coworkers presented their research on the coupled dipole method to predict nanoscale vdW forces.[50, 51] The vdW forces are important at the final stage of colloidal crystal formation for keeping the particles together and holding the structure.

Since the vdW interactions are always present and usually attractive, there must be a counter-force existing between the colloidal particles to keep them suspended as individual particles in the dispersion media, which often is the electrostatic repulsion (Fig. 2). Electrostatic forces between particles are usually more complex than simple Coulomb interactions between particles, although the heuristic remains essentially true like-charged surface repel and oppositely-charged surface attract. The electrostatic interaction energy model used to describe the commonly

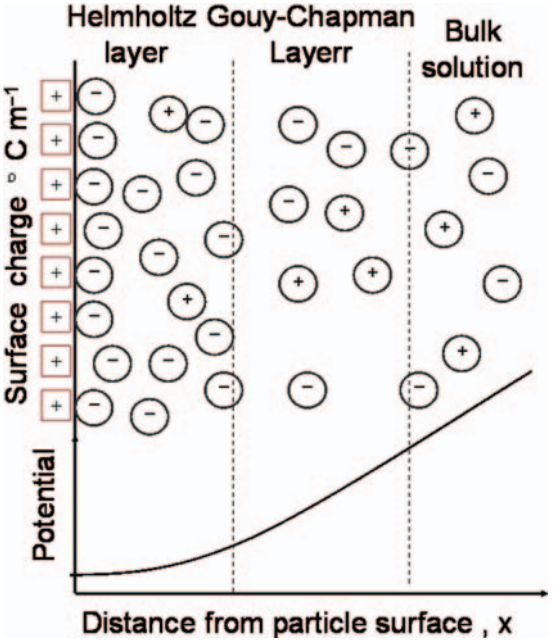

Fig. 3. An illustration of the Gouy-Chapman-Stern model for the electric double layer at the charged surface of a particle and the variation of potential.

encountered geometry of a sphere, 1, and a flat plate, 2, in water, is illustrated in Figure 3 and given by:[52, 53]

$$\Delta G_{1w2}^{EL} = 64\pi\alpha\varepsilon\varepsilon_0\left[\frac{kT}{ze}\right]^2\beta_1\beta_2\exp(-\kappa h) \quad (2)$$

where $\beta_i = \tanh[ze\Psi_0/(4kT)]$, α is particles radius, ε is dielectric constant of the medium, ε_0 is permittivity in a vacuum, $C_2/J\cdot m$, k is Boltzmans constant, 1.38E−23 J/°K, T is temperature, °K, z is valence of electrolyte, e is electron charge, 1.602×10^{-19}C, ψ_0 is surface potential, d is separation distance, κ is reciprocal of the Debye length, m^{-1}, the reciprocal of the Debye length, $\kappa=\sqrt{(1000e_2N_A/\varepsilon kT)\sum_i z_iM_i}$, N_A is Avagodro's Number, 6.02×10^{23} molecules/mol, M_i is molar concentration of electrolyte, mol/L.

It is noteworthy that the electrostatic forces have two opposite impacts on the ordering of nanoparticles. An appropriate repulsion is necessary to prevent irreversible agglomeration, and reduce structural defects under the Brownian motions. On the other hand, an inevitable reconstruction due to the solvent-dependent repulsion might destroy the once ordered structures.[54] Obviously, the disordering effect becomes more prominent with the increase of the particles assembly structure.

According to relationship (2), changes of electrolyte concentration and pH result in change in electrostatic interaction energy. At a specific salt concentration, the electrostatic interaction force can be virtually neutralized. At a surface specific pH, reactions between protons and surface functional groups can result in a net surface potential that

approaches zero. The electrostatic screening is very important for asymmetric electrostatic forces, since the forces are often localized to regions on the particle surfaces of dimension roughly 10 times Debye length. The screened electrostatic repulsion by addition of salt gives the particle monolayer of smaller domain and more defects. The more particle charge by higher pH results in the more improved array quality.[55, 56] The electrostatic interactions play a dominant role in the charged spherical particles system, which in fact represent 2D counterparts of the 3D crystals from charged spherical particles.

The necessity of repulsion in forming ordered colloidal crystals has been demonstrated by 2D colloidal crystal formation at the air-water interface through varying the ionic strength of the aqueous solution, which in turn changes the charging condition of the colloidal particles.[57] The investigation from Okubo and coworkers[58] indicated that the microstructure dependence on the inter-particle repulsion originated from a leap in the frequency of inter-particle collision at a critical surface coverage value of $\Phi_C \approx 0.65$, and the stronger inter-particle repulsion and weaker particle–substrate attraction were preferable for the better microstructure above the critical Φ_C of about 0.6. The use of electrostatic forces in non-aqueous media has a clear difference from that in aqueous media. Since the Debye length in non-aqueous media is usually much larger than the particle radius, site-specific assembly in non-aqueous media is difficult.

Self-assembly on templates driven by electrostatics force presents an intriguing candidate for dynamic control because of the ease at which the driving electric force can be applied and manipulated on a template. However, a major barrier towards the use of dynamic electrostatic forces in assembly is the difficulty in controlling the charge on individual freestanding micro-components and in preventing the assembly of multiple components to the same binging site.

2.3. Steric Forces and Depletion Forces

Polymers have a tendency to adsorb on suspended particles in solution, forming layers 10 to 20 nm in thickness so that they serve to stabilize neighboring particles by steric interactions. Steric interactions are those adsorbed chains and/or chain elements. They can be defined quantitatively in terms of the energy change occurring upon interaction of the adsorbed layers, as illustrated in Figure 4. Steric interactions can be attractive or repulsive. The greater steric repulsion generated by the addition of polymers moves the minimum in the potential energy curve, and thus reduces the overall viscosity (Fig. 4(b)). The presence of the steric repulsion allows the particles to pack closely and reversibly much like hard spheres.[55, 59–63]

The physical basis of the steric repulsion is a combination of a volume restriction effect arising from the

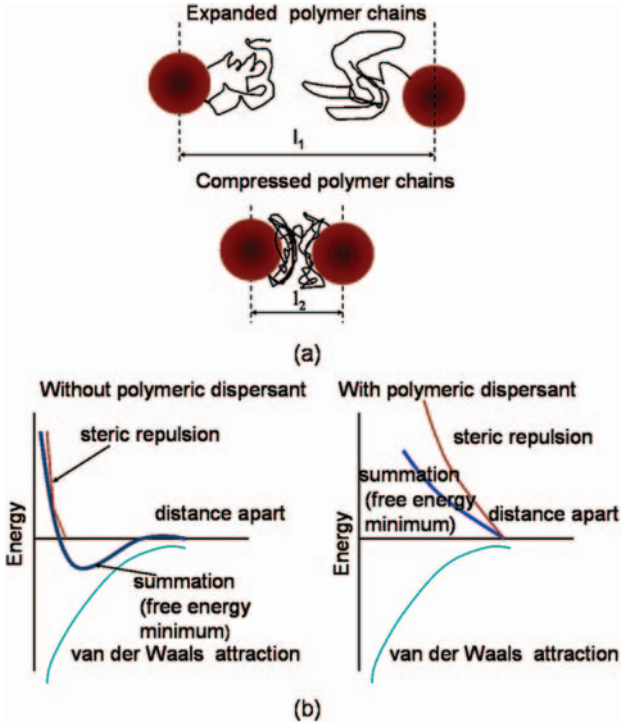

Fig. 4. (a) Schematic of entropic contribution to steric interactions. Reprinted with permission from [39], D. Grasso et al., *Rev. Environ. Sci. Biotechnol.* 1, 17 **(2002)**. © 2002, Kluwer Academic Publishers, and (b) potential energy curve (from http://www.inkline.gr/inkjet/newtech/tech/dispersion/).

decrease in possible configurations in the region between the two surfaces and an osmotic effect due to the relatively high concentration of adsorbed polymers in the region between the two surfaces as they approach one another. Steric forces between surfaces coated with polymers depend on several factors, such as the quality of the solvent, the attachment of the polymer to the surface, etc. Recently, the colloidal probe technique[64] and the atomic force microscope[65] have been employed to probe steric interactions between adsorbed polyelectrolytes. Solvent quality can dictate the strength of repulsion and the separation distance between closely packed particles. Judicious selection of the ligand moieties can allow covalent linkage by chemical reaction or biospecific interactions between closely situated neighboring particles, locking in their architecture.[66–68]

Depletion interactions can occur in systems that have particles with multimodal size distributions in solution. Forces can arise due to local differences in species concentrations. Geometric exclusion of the smaller species from the gap between larger particles causes an osmotic pressure which results in an attractive force between the larger particles. Thus, the larger particles are drawn together by the maximization of entropy between the smaller species. In this way, size selective segregation and aggregation can be reversibly controlled by addition of these smaller species.[34, 69] Depletion forces for colloidal

REVIEW

particles are well-understood, both theoretically[70, 71] and experimentally.[72–74] A more challenging topic with depletion forces arises when the depletant molecule or nanocolloid is of a comparable size to the particles on which they are applying a force. Asakura and Oosawa[75] calculated the depletion interaction between two spherical particles suspended in solutions of coiled chain macromolecules and charged spherical macromolecules. They showed that the depletion force in the presence of polymer chains can be much greater than in solutions of spherical molecules.

Schweizer and coworkers[76] have developed the PRISM model for predicting depletion forces when the surrounding polymer is comparable or larger in size than the nanocolloids. Bowen and Williams[77] measured depletion forces between a polystyrene sphere and a glass slide and modeled the depletion attraction changes in osmotic pressure. Mason[78] has used depletion forces for disk-shaped particles to direct the assembly of stacks of clay disks, and Stroock and co-workers[79] have similarly used depletion forces to assemble short cylinders with flat ends. Wostyn and Velev[80, 81] have shown that depletion interaction between binary mixtures of large and small colloidal microspheres can be used to assemble colloids into crystalline lattice structures. An advantage in using depletion forces for assembly is that the interaction potentials are easily controlled in the weak-attraction regime (1 to 5 kT).

2.4. Hydrophobic Forces and Hydrogen Bonding

Hydrophobic forces are actually due to entropic contributions which seek to minimize the entropy drop which occurs during the formation of molecular complexes near hydrophobic surfaces. The hydrophobic interaction can be quite strong, often stronger than vdW attraction. Hydrogen-bonding force results in hydrophobic interactions, the hydration pressure results in hydrophilic interactions. Experimental studies have found that the hydrophobic force law between two macroscopic hydrophobic surfaces is of surprisingly long range, decaying exponentially with a characteristic decay length of 1–2 nm in the range 0–10 nm.[48] However, at separations greater than 10 nm, some experiments have shown that the attraction does depend on the intervening electrolyte in dilute solutions, or solutions containing divalent ions, it can continue to exceed the vdW attraction up to separations of 80 nm.[82, 83] Hydrophobic forces have been localized on particles. By alternating the pH to create local regions of hydrophobic and hydrophilic forces, assemblies have been created.[84, 85] Anisotropic hydrophobic forces have also driven the assembly of CdTe sheets.[86] A much more common use for hydrophobic forces in assembly is in the exploitation of surface tension, which is an extremely strong tension, often during a drying process. It is currently the most common force used in particle assembly.

The effect of hydrogen "bridges" and weak bonds on certain properties of substances had been observed by many early investigators.[87] Hydrogen bonds can vary in strength from very weak (1–2 kJ mol^{-1}) to extremely strong (>155 kJ mol^{-1}), but sufficiently greater than kT to mediate intra- and intermolecular assemblies.[88] Hydrogen bonds are not specific to water, and can occur between electronegative atoms, such as O, N, F, Cl and hydrogen atoms covalently linked to other similarly electronegative atoms. In addition, hydrogen bonding can also occur between water molecules and organically coated solid material, as illustrated in Figure 5. The typical length of a hydrogen bond in water is 1.97 Å. Colloidal nanoparticles interactions in environmental systems most often take place in the presence of water molecules in where the propensity of molecules to hydrogen bond with itself or other moieties in solution or on surface. Hydrogen bonding may affect surface properties and colloidal behavior in aqueous media.

2.5. Capillary Forces

Capillary forces are long range interactions between particles mediated by fluid interfaces. They take place at the three phase boundary of the solid particles, the suspending liquid and a mobile gas, where form the meniscus of evaporation liquid film, with an effective range of up to several millimeters depending on the surface tension, contact angle, and particle size and density. The primary origin of capillary force is the surface tension of the suspending liquid, which tends to minimize its total surface energy in contact with a non-miscible mobile phase by appropriately deforming the liquid surface between the solid particles.[34, 89]

The capillary forces are classified by normal forces and lateral forces.[34] The normal capillary forces result from either liquid-in-gas or gas-in-liquid capillary bridges, which lead to particle-particle and particle-wall interactions. The forces are directed normally to the contact line. The normal capillary-forces can be attractive or repulsive depending on whether the capillary bridge is concave or convex. The attractive forces of this type can lead to three-dimensional aggregation and consolidation of bodies built

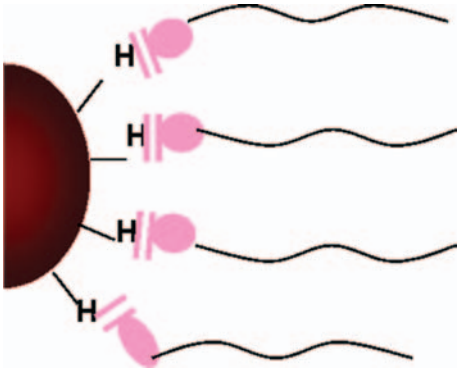

Fig. 5. Hydrogen bonding to a particle and a polymeric group.

up from particulates. The lateral capillary forces are the results of the overlap of perturbations (menisci) around two particles. The forces are parallel to the contact line. They could be also attractive or repulsive depending on whether the overlapping menisci formed around the two particles are similar (both concave) or dissimilar (one is concave and the other is convex).[34, 90] The attractive lateral capillary forces cause two-dimensional aggregation and ordering in a rather wide scale of particle sizes from 1 cm to 1 nm.[34]

The lateral capillary force has two fundamental forms, capillary flotation force and capillary immersion force, as illustrated in Figure 6.[34] The flotation capillary force interfacial deformation results from the interplay between the particle weight, buoyancy and surface tension when particles float at the air-liquid interface. The flotation capillary force is important in colloidal self-assembly at the air-water interface. The immersion force interfacial deformation is related to the wetting properties of the particle surface to the position of the contact line and the magnitude of the contact angle, rather than to the particle gravity and buoyancy.[34] When particles are located on a planar solid wall and are partially immersed in a liquid film with the thickness in the range of the particle size. The immersion force is one of the main factors causing the self-assembly of small colloidal particles.

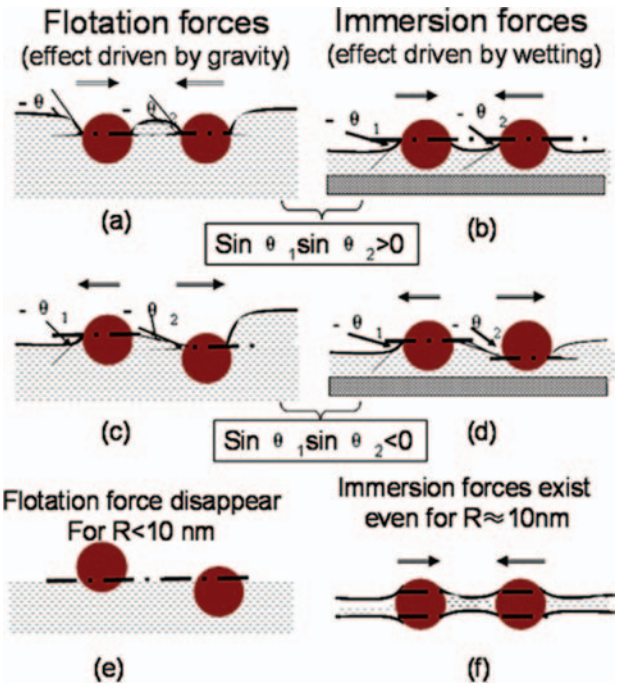

Fig. 6. An illustration of comparison between the flotation (a, c, e) and immersion (b, d, f) lateral capillary forces. θ_1 and θ_2 are meniscus slope angles, The flotation force appears between freely floating articles where the immersion force appears when particles are partially immersed in a liquid film. Reprinted with permission from [90], P. A. Kralchevsky and K. Nagayama, *Langmuir* 10, 23 (**1994**) © 1994, American Chemical Society.

The flotation and immersion forces can be both attractive (Figs. 6(a and b)) and repulsive (Figs. 6(c and d)).[34] This is determined by the signs of the meniscus slope angles θ_1 and θ_2 at the two contact lines: the capillary force is attractive when $\sin\theta_1 \sin\theta_2 > 0$ and repulsive when $\sin\theta_1 \sin\theta_2 < 0$. In the case of flotation forces $\theta > 0$ for light particles (including bubbles) and $\theta < 0$ for heavy particles. In the case of immersion forces between particles protruding from an aqueous layer, $\theta > 0$ is for hydrophilic particles and $\theta < 0$ is for hydrophobic particles. When $\theta = 0$ there is no meniscus deformation and, hence, there is no capillary interaction between the particles. This can happen when the weight of the particles is too small to create a significant surface deformation, Figure 6(e).

For the systems depicted in Figure 6, the lateral capillary force is given:[34, 91]

$$F \approx -2\pi\sigma Q_1 Q_2 q K_1(qL) \quad (r_K \ll L) \tag{3}$$

where $q = \sqrt{\rho g/\sigma}$ is the reverse capillary length, g is the gravitational acceleration, ρ is the liquid density and $\sigma$is the surface tension. $Q_i = r_i \sin\Psi_i$ $(I = 1, 2)$ is the so called capillary charge, r_i and ψ_i are the radii of the contact line and the slope angle at the contact line of the respective particle. K_1 is the modified Bessel function of the second kind. L is the distance between the centers of the two particles.

Equation (3) has a simple asymptotic formula when L is much smaller than q^{-1}:

The approximate expression for the lateral capillary force can be written:[34]

$$F \approx -2\pi\sigma Q_1 Q_2 / L \quad (r_K \ll L \ll q^{-1}) \tag{4}$$

The flotation and immersion forces exhibit similar dependence on the inter-particle separation, however, very different dependencies on the particle radius and the surface tension of the liquid due to the different magnitudes of the corresponding capillary charge. When the interfacial tension increases the flotation force decreases, while the immersion force increases.[90] The flotation force decrease with the decrease of sphere radius R much more strongly than the immersion force. So the flotation force is negligible for $R < 5$–10 μm, whereas the immersion force can be significant even when $R = 2$ nm.

In fact, in the large-area well-ordered structure formation the capillary interactions among particles are a multi-body problem due to the multiple neighbors of each colloids and the long-range effect of the capillary force. In this case, a quantitative estimation of the net capillary effect is complex to solve. The simulation studies for the self-assembly process of colloidal particles due to capillary immersion force have been reported and further explained the formation of particles.[92–94] A comprehensive review of various types of capillary forces on particle structuring have been reported by Karlchevsky and Denkov.[34]

The capillary force have been utilized for the self-assembly of micro- and nanoparticles to generate simply and intricate structures.[73, 74, 95–97] Denkov and coworkers[96] revealed the mechanism of array formation from micrometer-size latex particles on glass substrate. The dynamics of 2D ordering of micrometer-size polystyrene latex spheres on a horizontal glass substrate has been directly observed by means of optical microscopy. It turns out that the ordering starts when the thickness of the water layer containing particles becomes approximately equal to the particle diameter. By variation of the electrolyte concentration, the charge of the particles, and their volume fraction, it is proven that neither the electrostatic repulsion nor the vdW attraction between the particles is responsible for the formation of two-dimensional crystals. The direct observations revealed the main factors governing the ordering-the attractive capillary forces and the convective transport of particles toward the ordered region. The control of the water evaporation rate turns out to allow obtaining either well-ordered monolayers or multilayers.

As shown in Figure 7, the capillary force assembly mainly focuses on four aspects:
(1) Self-assembly of spherical or non-spherical particles in wetting films;

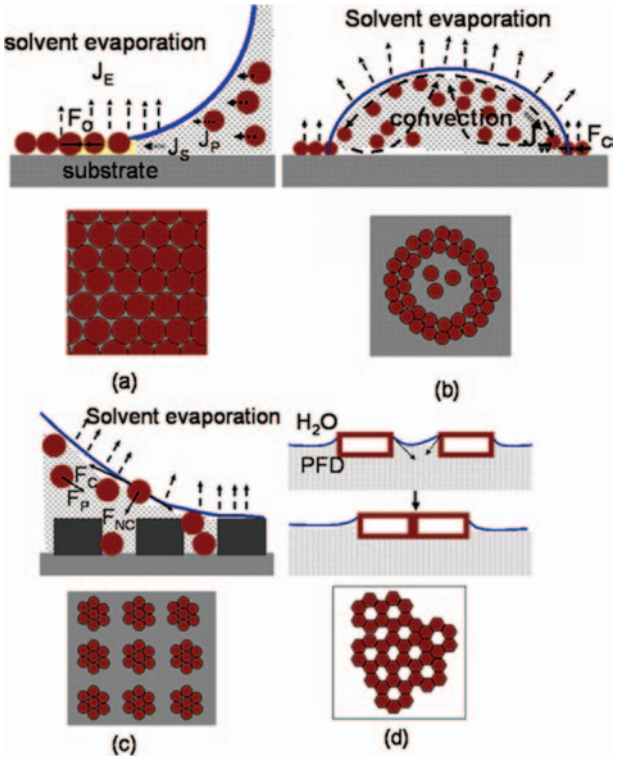

Fig. 7. Schematic of the self-assemby of particles under the action of capillary forces and structures. (a) Self-assembly of spheres by convectively coating to fabricate to closely-packed monolayer or multilayers; (b) by evaporating drops of suspensions to fabricate circular particulate rings on substrate; (c) self-assembly of particles on patterned substrates to fabricate expected structures; (d) the meso-scale self-assembly of particles.

(2) Formation of balls and rings of by evaporating drops of suspensions;
(3) Self-assembly of particles on patterned substrates or in capillary networks;
(4) The meso-scale self-assembly of particles.

2.6. Viscous Force, Friction Force and Gravitational Force

Particles are subjected to viscous force from fluid when they move in the fluid (Fig. 8). This viscous force for a particle moving in an infinite liquid can be expressed as follows:

$$F_v = -3\pi\eta D v = -\beta v \tag{5}$$

where η is the viscosity of the liquid, D is the diameter of the particle, v is the velocity of the particle, and β is the drag coefficient.

During the motion a particle on the substrate is also subjected of the force of the friction between particle and substrate (Fig. 8). It can be expressed as follows:

$$F_f = -\mu(mg + 2\pi\gamma Q) \tag{6}$$

where m is the particles mass and μ is the friction coefficient. The first term in the parentheses accounts for the normal load due to the particle weight. The second term is a contribution from the vertical projection of the surface tension. The first term is negligible for colloidal particles due to smaller than the second one.

The mobility of the particles during the particle array on the substrate should be retarded by the stronger particle-substrate attraction, which results in less particle order. So the surface treatment of the substrate is a good way to increase the particle order. The increase in the hydrophilicity of the substrate through the surface treatment is attributed to the removal of contamination and increases in the number of hydrophilic group on the surface and further enhances the attraction between the substrate and particles. In addition, particle surface roughness also has a little effect on the array of particles. It is worthwhile noting that at some cases for the self-assembly of the particles on the substrate, the friction with the substrate is negligible. The main hydrodynamic resistance comes from the viscous friction in the liquid film.[96]

Gravity is almost negligible in the colloidal system where surface adhesion, electrostatic and vdW forces dominate, while it ubiquitously present and is one of useful

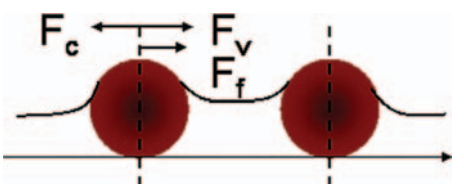

Fig. 8. Two particles trapped in a thin wetting film and moving in front of each other due to the applied forces.

forces in driving mechanism for self-assembly of micro-size particles. The strength of gravity relative to surface forces decreases as the size decreases. Gravitational forces differ, however, by being always attractive, never repulsive, and by being inherently weaker, with the electrostatic repulsion between two protons being three orders greater than their gravity. The gravity similarly exhibits an inverse square dependence on distance between two point masses:

$$F = G\frac{m_1 m_2}{r^2} \tag{7}$$

where F is the magnitude of the gravitational force between the two point masses, G is the gravitational constant, m_1 is the mass of the first point mass, m_2 is the mass of the second point mass, is the distance between the two point masses.

Sedimentation in a gravitational field, from dispersions, is the natural way to produce particles arrays among other methods of self-assembly. However, the sedimentation procedure is not that simple and comprises several processes such as gravitational settling, Brownian motion, and crystallization, including both nucleation and growth stages. Sedimentation self-assembly was applied to form photonic crystals with silica colloids or zinc oxide colloids. In addition, the use of gravity and complimentary-shaped wells has lead to a fluidic self-assembly process.[98–99] Gravitational force-based assembly methods have demonstrated the highest assembly rate to date.

3. COATING PROCESSES

3.1. Dip Coating

3.1.1. Dip Coating Processes and Principles

The dip coating technique is one of the most popular wet coating methods in fabricating coatings from colloidal suspensions and sol–gel solutions on substrates. The substrates could be flat panels, cylinders or complex geometries. It can operate in either continuous or batch modes. The dip coating technique can be simply described as a process where the substrate to be coated is immersed in a liquid and then withdrawn with a well-defined withdrawal speed under controlled temperature and atmospheric conditions.

Scriven[100] described the dip coating technique as five stages: immersion, start up, deposition, drainage and evaporation, as shown in Figure 9. In the dip coating process, the particles self-assembled into ordered structure on substrate as substrate is slowly drag upward from suspension. The thickness of the coating is determined by a complex competition between six forces during the coating deposition stage: (1) viscous drag upward on the liquid by the moving substrate, (2) force of gravity, (3) resultant force of surface tension in the meniscus, (4) intertial force of the boundary liquid layer, (5) surface tension gradient, and (6) pressure.

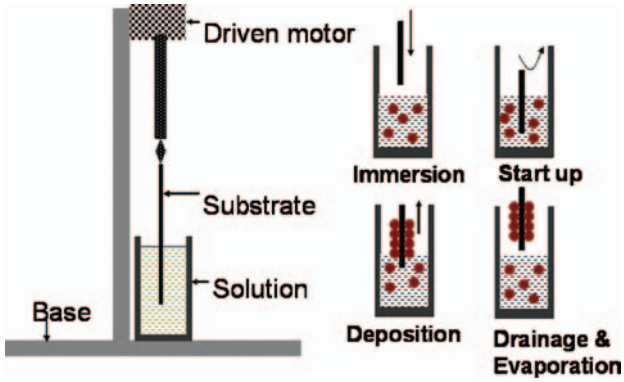

Fig. 9. Schematic of the setup and process of dip coating: immersion, start up, deposition, drainage and evaporation.

If the withdrawal speed is chosen such that the sheer rates keep the system in the Newtonian regime, the coating thickness can be calculated by the Landau-Levich equation:[101]

$$h = 0.94 \cdot \frac{(\eta \cdot v)^{2/3}}{\gamma_{LV}^{1/6}(\rho \cdot g)^{1/2}} \tag{8}$$

where h is coating thickness, v is viscosity, r_{LV} is liquid-vapore surface tension, ρ is density, and g is gravity.

In the dip coating process, the self-assembly of particles occurs at the meniscus region between liquid and gas interfaces formed by withdrawing the substrate. Solvent evaporation from the local menisci around the particles induces a convective flux of solvent and particles from the bulk move towards the upper region of the substrate to the nuclei, continuing the growth of the crystal structure that is schematically depicted in Figure 10.[102] As the meniscus of the suspension sweeps the substrate, a conformal crystalline monolayer is formed on the substrate. The mass-transfer process simultaneously occurs over the entire substrate, ensuring a high process throughput. Many factors contribute to determining the final state of particle-assembly. By controlling the withdrawal speed, submersion time, number of dipping cycles,

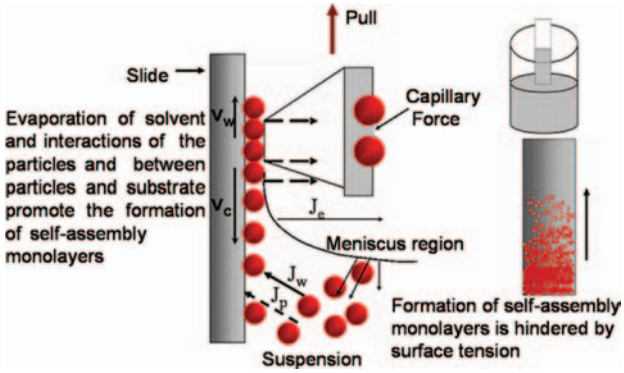

Fig. 10. Schematic of the mechanism of self-assembly by dip coating.

solution composition, concentration and temperature, solvent, substrate, and environment humidity, a large variety of repeatable dip-coated particle-assembly structures and thicknesses can be fabricated.

The mechanism of dip coated particle-assembly has been revealed to some extent due to the development of the convective coating technique because the dip-coated particles assembly can be regarded as a class vertical convective assembly process.[103] We will discuss it in detail in Section 3.3.

For the formation of well-ordered monolayers, at the proper experimental conditions, the upper region of the meniscus retreats below the height of the particle monolayers as the solvent evaporates, exposing the particles surface as interfaces. At this moment, the vertical component of capillary forces drags the partially immersed particles downward to the substrate surface where particles self-assembly into ordered monolayer structures (Fig. 10). The dip coating process normally leads to the formation of hexagonal structures. In the cases of the higher particle concentration or slower withdrawal speed or fasted evaporation rate, the meniscus height is larger and results in large convective flux so that thicker coatings can be deposited.[96] Contrarily, the smaller meniscus height results in small convective flux, so the non-connected coatings are formed.[102, 103] The meniscus height can be taken as intermediate between those for coatings of one and multilayers of particles formed on the substrates.

Generally, the dip coating method does not allow a sufficient control over either the surface morphology or the uniformity on the entire substrate due to rheological properties of the colloidal suspensions and the gravitational field. The final morphology and microstructural characteristics of the particle assembly are usually affected by the particle characteristics (size, density and position), solvent characteristics (viscosity, evaporation rate) as well as substrate conditions (temperature, roughness, and chemistry) and environmental conditions.

3.1.2. Application and Development

The dip coating technique is a simple, fast, versatile, cheap approach in fabrication of the colloidal particles coatings and the sol–gel thin films which applied to various fields.[104–107] Usually the deposition operations of the dip coating are completely automated by control system. The control of layer thickness can be realized by Landau-Levich's Eq. (8) with high precision. Dip coater customers are found worldwide in both academia and industry. A angle-dependent dip coating process has been developed.[108] The traditional dip coating technique has preponderance in fabricating of colloidal nanoparticle coatings and sol–gel thin films which not require accurately controllable, well-ordered structures. However, there are several conundrums in the fabrication of colloidal nanoparticle coatings and sol–gel thin films: (1) improvement of the density of films, (2) non-defects and crack-free thin films, (3) handling large panes and the stability of the dip coating baths under atmosphere conditions, (4) coating on one side of substrate. Therefore, it should be of great interest and technological importance to explore new materials and procedure.

It is a challenge to fabricate the uniform, well-ordered and controllable self-assembly structures on large area substrate by the traditional dip coating technique. Recently, we have succeeded in fabricating the self-assembled monolayers of micro-sized silica spheres as antireflective films on glass and silicon wafer by dip-coating.[102] Record large area of uniformly coated structures were formed with dimensions of 3×10 mm^2 and 1.5×11 mm^2 on the silicon and glass substrates, respectively. Shown in Figure 11 are the scanning electron micrographs (SEMs) taken in the same location but at different magnification scales. The array is hexagonal structure with 6-fold symmetry, and looks sufficiently uniform and close-packed. In our experiments, the coating area is limited by the volume of solution and the properties of solution (plain silica microspheres in water or ethanol without any organic compounds) and substrate (without any surface treatment). At the same time, we also have succeeded in fabricating the alternately stacking layers of inorganic nanoparticles of different refractive indices to form the distributed Bragg reflectors on the silicon and glass substrates by dip coating.[109] The SEM and the atomic force microscope studies confirm thickness uniformity achieved along the fabrication direction, and a good quality of surfaces and interfaces. By controlling the withdrawal speed, submersion time, and particles concentration, we can adjust the thickness of coating, so that the peak reflectance region can be tuned from the blue-green to the infrared portion of the electromagnetic spectrum. It is worth while pointing out that we still did not give organic compounds and substrate treatment. In this case, the coatings have good optical quality.

Ko and coworkers[103] fabricated self-assembled monolayers of monodispersed silica submicrometer particles and used them as lithographic mask. Nagao and his coworkers[110, 111] fabricated the submicrometer silica and polystyrene particle monolayers with high regularity via the modified dip coating approach. Additionally, the honeycomb structure of silica particles under monolayered

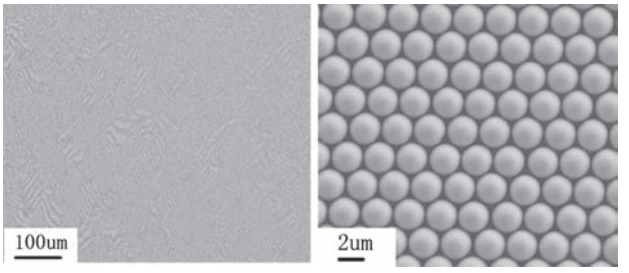

Fig. 11. SEM images of monolayer of silica microspheres by dip coating with different magnifications.

polystyrene particles was also fabricated with double dip coating of these particles. Repetition of the dip coatings is applicable to multilayer particles with different sizes. The results demonstrated that the dip coating technique is applicable to ordering particles under the polymer sheets. Two important factors for arrangement of the particles are the low ionic strength and the proper particle concentration[111] Bormashenko and coworkers[112] also obtained self-assembled microscaled photonic crystal films in which contain dispersed hexagonally packed holes on the polymer piezoelectric substrates by a fast dip coating process. They suggested that evaporation and boiling of the solvent played a decisive role in the simultaneous formation of bubbles in the evaporated films' bulk and mesoscopic pattern formation. Fabricated structures have a potential as 2D tunable photonic crystals.

The dip coating technique also can be applied to patterned particle arrays. Yang and coworkers[113] reported the fabrication of nanowire patterning by dip coating. By programming the stick–slip motion of the solvent contact line during dip coating, selective positioning of nanowire arrays with controllable density and spacing can be achieved. Comparing to other patterning methods, their method starts directly from a nanowire dispersion and the minimal material consumption. The nanowire dispersion can be readily reused for future deposition by adding more solvent to compensate for evaporation. The results demonstrate the potential of controlled dewetting for patterning nanostructures. However, it should be noting that the immersion methods for patterning colloid particles are relatively slow and require a large volume of colloidal solution. Uniform filling of open, continuous channels or networks with colloidal crystals can prove difficult because of channel plugging problems during capillary-driven infiltration of suspension.

Generally, the traditional dip coating technique has preponderance in fabricating of colloidal particles coatings which not require accurately controllable and well-ordered structures. However, this process has difficulty in producing uniform well-ordered particles structures on a large area substrate in the effective time. A large volume of particles solution is required to immerse the substrate completely and consume more solution for double-side coating. It seems to be diametrically opposed to develop large-scale process with low cost. These conundrums have been addressed to some extent by many recent works describing the fabrication of self-assembly structures by vertical convective coating technique and one-side coating method.

3.2. Spin Coating

3.2.1. Spin Coating Processes and Principles

The spin coating technique utilized in various academic and industrial applications, is one of the most established wet coating methods. It is a simple, convenient, cheap, one-side, material saving, rapid and highly reproducible method to produce homogeneous films on a rigid flat or slightly curved substrate. In the spin coating process, the substrate spins around an axis that should be perpendicular to the coating area. Bornside and coworkers[114] divided the process into four stages: deposition, spin-up, spin-off, and evaporation, as shown schematically in Figure 12. The first three stages are sequential, while the fourth normally proceeds throughout the coating process. Both of spin-off and evaporation are the two stages that have the most impact on final coating thickness. The quality of the coating depends on the rheological parameters of the coating liquid. Another important parameter is the Reynolds number of the surrounding atmosphere.[115] Here the material which should be deposited is present in form of a viscous solution, which is applied onto the surface. Slow spinning distributes the viscous material over the entire surface, whereas the quick spinning defines the final thickness of the material on top of the substrate.

The thickness of a spin coating is the result of the delicate transition by which evaporation takes over from spin-off. Meyethofer[116] described the dependence of the final thickness of spin coated layer on the processing and materials parameters like angular, velocity, viscosity and solvent evaporation rate by the semiempirical formula:

$$d = \left(1 - \frac{\rho_A}{\rho_{A_0}}\right) \times \left(\frac{3\eta \cdot m}{2\rho_{A_0} \cdot \omega^2}\right)^{1/3} \quad (9)$$

The film thickness can be adjusted by varying the rotation speed, the rotation time, and the concentration of the used solution. The film thickness can be affected by the formation of a "skin" layer during the coating process.[117]

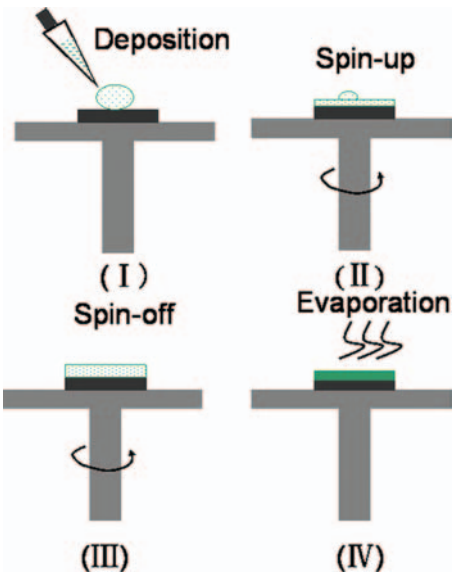

Fig. 12. Schematic of the process of spin coating: deposition, spin-up, spin-off, and evaporation.

Skin layer formation is caused by the difference in the properties of the spinning material near the air interface and the bulk fluid. A separate drying step is sometimes added after the high speed spin step to further dry the film without substantially thinning it. This can be advantageous for the thick film since long drying times may be necessary to increase the physical stability of the film before handling.

The spin coating differs from the dip coating in that the deposited film becomes thin by the centrifugal draining. and tends to be uniform due to the balance between the centrifugal force which controlled by spin speed and drives flow radially outward and viscous forces (friction) which are determined by solvent viscosity and acts radially inward. Even with non-planar substrate very homogeneous thickness can be obtained. The disadvantage of this method is that it is limited by the solvent and that no lateral resolution is possible.

The spin coating assembly of particles can also be regarded as a class of evaporation driven self-assembly techniques. In general, for the spin coating assembly of particles, the first stage is the spread across the wafer of the droplet including the coating particles driven by the viscosity and the centrifugal forces. The second stage is the formation of the well-ordered particles array driven by the solvent evaporation, as shown in Figure 13. Early results show that the complete wetting of the substrate by the colloidal dispersions is critical to obtain uniform monolayer on a large area substrate. By using the spin coating, one can rapidly fabricate monolayer of particle assemblies over a large area on various kinds of substrate. However, the ordering of particles is still unsatisfactory and needs to be improved by contriving the drying process of the solvent during coating.

3.2.2. Application and Development

For over two decades, the spin coating has been employed to form 2D colloidal crystals quickly.[21, 118–125] The dispersion of micro- and nanoparticles without binder is spin-coated on a solid substrate and matrix-free close-packed nanoparticle assemblies were successfully obtained in some cases.[125–127] Okuyama and coworkers[128] reported that they fabricated monolayers of silica particles of 550 nm and 300 nm with relatively surface coverage of 72 and 70%, respectively, on a 2 in. diameter sapphire substrate using a spin coating. It is obvious that the substrate treatment and the two-step spin coating technique play important roles in the obtaining the high surface coverage with the monolayers of silica particles in their study. Additionally, the controlling of experimental parameters, such as solution concentration, ambient humidity and spin speed, to keep a balance between spin speed and solvent evaporation rate is an important factor in the fabrication of high-packed silica particles monolayers. By using a stepwise spin-coating process, Wang and coworkers[118] were able to fabricate silica spheres binary colloidal crystals with LS_2 or LS_3 structures by controlled the diameter ratio of big sphere to small spheres and spin coating speed.

The spin coating assembly allows the formation of ordered patterns of nanoparticles with controlled thickness and transverse patterns within confined photoresist pattern templates on an otherwise flat substrate[129] Ozin and Yang[130] produced opal-pattern chips on patterned silicon wafers by spin-coating. Brueck and Xia[131] prepared the directed assembly of silica nanoparticles (≦100 nm diameter) into 1D and 2D period arrays on the flat surfaces using periodic photoresist patterns as templates for the conventional spin-coating process, as shown in Figure 14.[131] Following particle deposition, the patterns were removed by heating or by chemical treatment, leaving parallel arrays of lines and continuous cross networked particle arrays with empty cylindrical holes on a flat. The number of particle layers, the pattern period, and the line/space ratio are controllable by varying the process conditions. This method provides a flexible and versatile route to the fabrication of particle arrays on a flat surface, which have potential applications in optics, electronics, sensing, and as a masking step for templating more complex nanostructures. More mono-dispersed particle-size distributions should result in increased local order within the particle arrays. Figure 15 shows the FE-SEM images of 1D patterns (Fig. 15(a)) and 2D cross network pattern (Fig. 15(b)) of 78 nm silica particles with 500 nm period.[131]

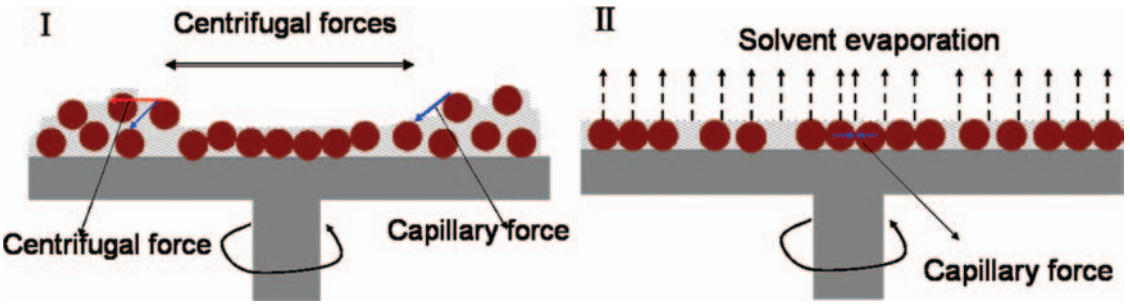

Fig. 13. Schematic of particles self-assembly by spin coating. (I) is the spread across the wafer of the droplet including the coating particles driven by the viscosity and the centrifugal forces, (II) is the formation of well-ordered particles array driven by the solvent evaporation.

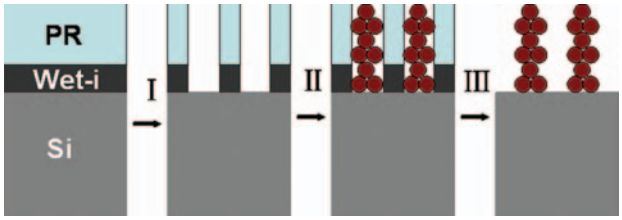

Fig. 14. Schematic illustration of deposition of patterned silica particles on planar surface using developing-soluble antireflecting coating (wet-i) layer: (I) expose using interference lithography and develop; (II) deposit silica particle using spin coating; and (III) strip off photoresist /wet-i. Reprinted with permission from [131], D. Xia and S. R. J. Brueck, *Nano Lett.* 4, 1295 (**2004**). © 2004, American Chemical Society.

Most recently, Jiang and coworkers[132–135] developed a procedure to prepare colloidal silica-polymer composite films based on spin-coating. In brief, silica colloidal spheres are first dispersed in a mixture of a viscous triacrylate monomer and a photoinitiator. The non-volatile dispersion is then spin-coated on a silicon wafer to obtain a thin layer. As the dispersion smears on the substrate, shearing induces 3D ordering of the particles in the monomer matrix, which is photpolymerized later on, providing mechanical stability for the structure. Selective removal of either the polymer matrix or the particles results in the formation of a direct silica or inverse polymer colloidal-crystal structures, respectively. Figure 16 shows schematic illustration of the fabrication procedures.

This approach enables rapid production of both 3D and 2D ordered colloidal crystals with remarkably large

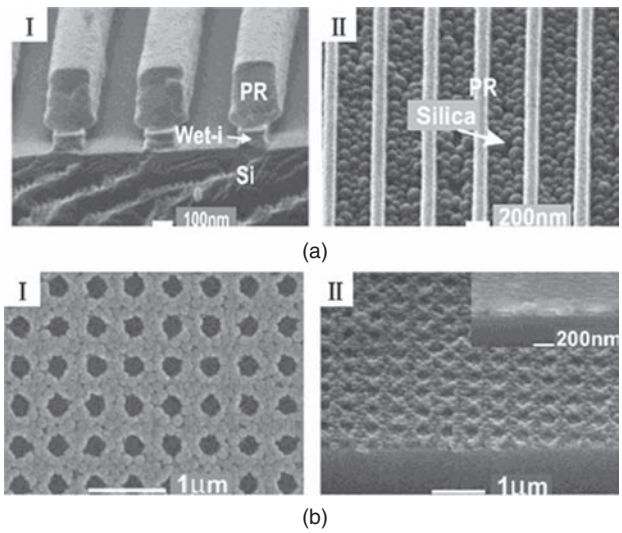

Fig. 15. (a) FE-SEM images of 1D patterns with 500 nm period. (I) PR/wet-i patterns at a cleaved edge. (II) ZL (78 nm diameter) silica particles confined between PR/wet-i walls. (b) The FE-SEM images of 2D cross network patterns of ZL (78 nm) particles with a 500-nm period. (I) top-view, (II) Tilted 45° view at a cleaved edge. Top right inset: magnified cross-sectional view. Reprinted with permission from [131], D. Xia and S. R. J. Brueck, *Nano Lett.* 4, 1295 (**2004**). © 2004, American Chemical Society.

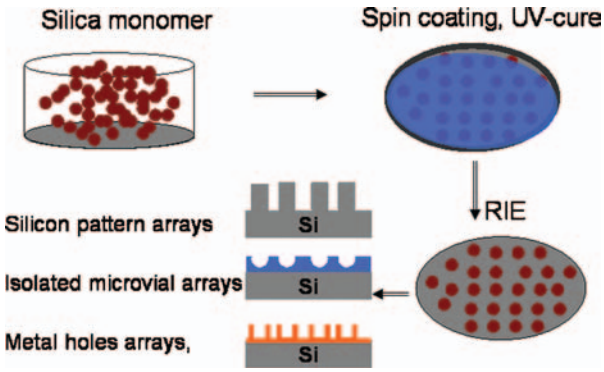

Fig. 16. Schematic illustration of the fabrication procedures of silica-polymer composite films by spin coating and the fabrication oof different structures.

domain sizes and unusual non close-packed structures. Figure 17 shows two typical structures from further processing of the colloidal silica-polymer composite films based on spin-coating.[132] One is the formation of wafer-scale colloidal crystals by selective removal of polymer matrix (Fig. 17(a)), and another is self-standing macroporous polymer replica after removal of silica spheres by wet etching (Fig. 17(b)). The formation of structures is attributed to shear-induced colloidal crystallization in which the high shear rate in the spin-coating process can lead to a sliding layer mechanism, in which 2D hexagonally packed colloidal layers are readily formed due to the coupling of the centrifugal and viscous forces.[136–142] The results indicated that the gradual increase of the spin speed was critical for the formation of high-quality monolayer colloidal crystal. This method provides a scalable templating nanofabrication platform for producing a large variety of microstructured materials with submicrometer-scale periodicity, such as macroporous polymers and nanocomposites,[132] sub-100 nm periodic nanostructures,[143] metal nanohole arrays,[144] 2D magnetic nanodots,[145] broadband antireflection coatings directly on crystalline silicon substrates,[146–148] and more. It is compatible with standard semiconductor microfabrication, enabling the large-scale productions of colloidal crystals for potential device applications. However, this technique still presents drawbacks that may limit its application, such as: (1) the use of the dense photopolymerized monomer leads to non-porosity and a very low refractive-index contrast, (2) limited to use in the crystallization of the different types of monodispersed latex particles, etc.

Mihi and coworkers[149] further improved Jiang's method and created thin silica and latex colloids colloidal-crystal films by spin-coating using a mixture of volatile solvents as dispersion media, allowing one to attain a strongly diffracting opal-like structure within minutes without further processing. The controlling of the medium that required a long time to evaporate allowing particles to order by shearing is one of key issues. Their method not only obtained planarized colloidal crystals with controlled

REVIEW

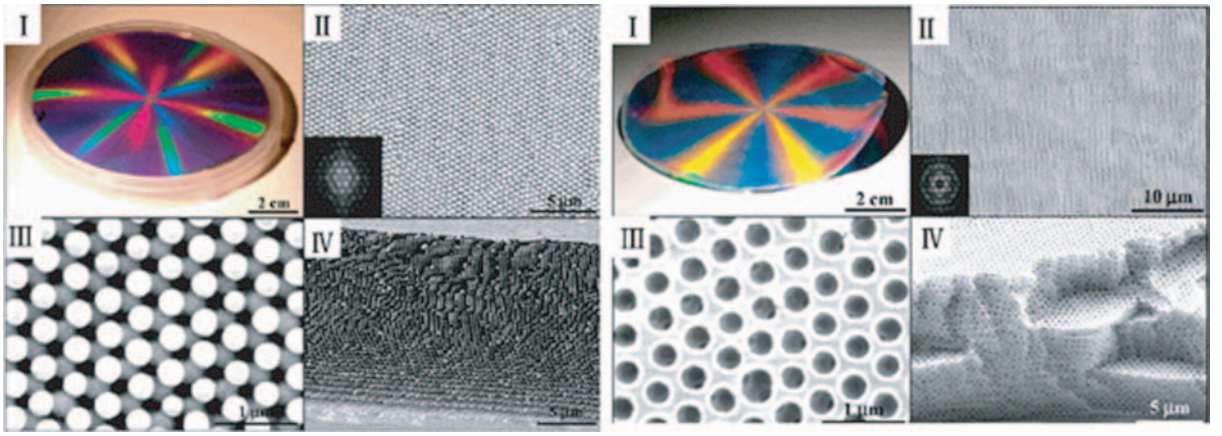

Fig. 17. (a) Formation of wafer-scale colloidal crystals by selective removal of polymer matrix. (I) Photo of a released colloidal crystal on a 4-inch silicon wafer. (II) Typical SEM image and its Fourier transform (inset) of the above sample. (III) Higher magnification image. (IV) Cross-sectional SEM image. (b) Self-standing macroporous polymer replica after removal of silica spheres by wet etching. (I) Photograph of a film placed on a 4-inch silicon wafer illuminated with white light. The wafer is only used for providing a dark background and a size reference. 325 nm silica sphere dispersion is spincoated at 600 rpm for 270 s to make the template. (II)Top-view SEM image and its Fourier transform (inset) of the sample in (I). (III) Higher magnification image showing interconnected inner pores. (IV) Side-view SEM image. Reprinted with permission from [132], P. Jiang and M. J. McFarland, *J. Am. Chem. Soc.* 126, 13778 (**2004**). © 2004, American Chemical Society.

REVIEW

thickness and good optical quality, but also to determine the crystal growth direction with respect to the substrate.

The spin coating technique has achieved rapid progress in the field of particle self-assembly. Lots of researches represents the spin coating is a faster and cheaper method for the fabrication of the large area well-ordered particles arrays or design structures with potentially industrial applications. However, the information regarding the effect of the parameters formation of the particle array as well as detailed data on the uniformity of the particles arrays over a large area of substrate and the extent of surface coverage is still insufficient.

3.3. Convective Coating

3.3.1. Convective Coating Processes and Principles

The convective coating is a novel fabrication method for controlled deposition of micro- and nano-particles. It was explored by Nagayama and coworkers.[150–153] and modified for a more scalable setup by Prevo and Velev.[69, 95, 154–156] Convective coating offers precise control and reduces materials consumption relative to standard dip coating or sedimentation techniques, although in some cases the convective coating process is similar to standard dip coating. It is feasible to fabricate monolayers of well-ordered close-packed micro- and nano-particle over large area at high rate of speed.

Convective coating is also called "evaporation-driven self-assembly, EDSA" or "convective assembly" because the self-assembly of particles are driven by capillary immersion force caused from the solution evaporation and hydrodynamic drag force, viz. After the particles protrude from the liquid film, attractive capillary immersion force emerges among the particles to result in well-ordered particle array. The typical setup and process of convective coating are illustrated in Figure 18.[154] The liquid suspension including coating particles injected into the wedge formed between substrate and deposition plate and is entrapped there by capillarity. The deposition plate is

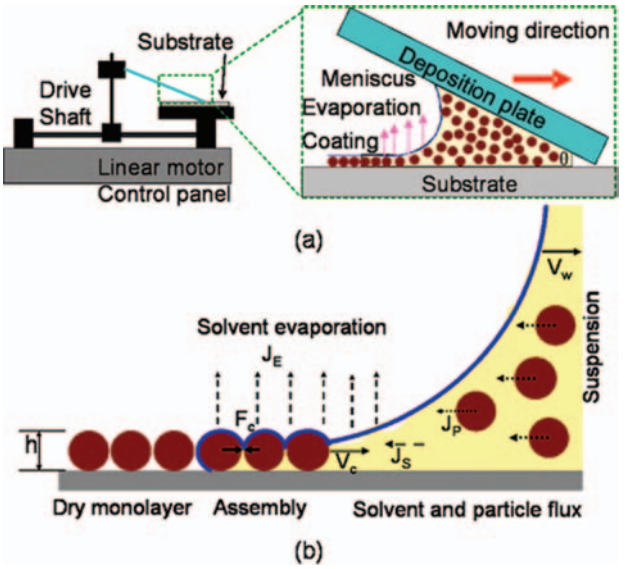

Fig. 18. (a) Schematic of the convective coating apparatus, the inset right illustrates the process of convective assembly driven by the evaporation flux, and (b) the drying region of a thin wetting film. The volumetric fluxes, J_P, J_S, and J_E are the particle flux, the solvent flux and the solvent evaporation flux, respectively. V_c and V_w are the rate of the array growth and the deposition of particles, respectively. The layer of thickness h is deposited at a growth rate V_c. Reprinted with permission from [154], B. G. Prevo and O. D. Velev, *Langmuir* 20, 2099 (**2004**). © 2004, American Chemical Society.

moved at a programmed speed, thus the liquid meniscus is dragged horizontally across the substrate surface. Particles are deposited from meniscus to substrate during the motion (Fig. 18(a)). The convective coating process including the particle flux J_P, the solvent flux J_W, and the solvent evaporation fluxes J_E, consists of nucleus formation and crystal growth of particle arrays on the substrate.[153] The particle flux drives the growth of particle arrays because the particles attach to the array's leading edge and remain there. The solvent flux compensates for the solvent evaporated from the particles arrays, and the particle flux causes particles to accumulate in the arrays, thus forming close-packed structures. Successive particle arrays are expected to be formed as the continuous particle flux fills up the space between the substrate and the film surface (Fig. 18(b)). The attraction to each other by the lateral capillary forces leads to the dense packing.

For steady state assembly process parameters and coating structural properties a simpler equation balancing the volumetric fluxes of the solvent and the accumulation of particles in the drying region has been proposed by Nagayama and Dimitrov.[152]

$$V_c = \frac{K\phi}{h(1-\varepsilon)(1-\phi)} \tag{10}$$

where K is a constant that depends on the relative humidity (or evaporative flux), ε and h are the porosity and the height of the deposited colloidal crystal, ϕ is the volume fraction of the particles in suspension, $1-\phi$ is the solvent volume fraction.

The well-ordered mono- and multilayers of particles can be obtained by appropriate control the shape of the liquid film surface, the liquid evaporation rate, particle concentration in the suspension, dispersed suspension volume, solvent, deposition plate rate, and wedge angle.[151, 157, 158] For the continuous formation of the 2D particle arrays onto a substrate plate, the deposition rate of the substrate should be equal to the rate of the array growth, $V_w = V_c$. When $V_w > V_c$ results in submonolayers consisted of small islands of several or tens particles were formed on the substrate. When $V_w < V_c$ leads to the formation of complete polycrystalline bilayers or multilayers, incomplete trilayers and multilayers on the substrate. In fact, the deposition rate of the substrate affects the shape of the meniscus which determines whether the particles assemble into a mono- or multilayer.[159, 160] Meanwhile, many more factors influencing the particle-surface interactions, such as surface topography and corrugation.[161–163] or even nanoscopic air bubbles[164] might have to be taken into account in order to completely understand the ordering phenomena of particles through capillary forces. Bedside, another important factor that should be considered is that during the drying process, the ionic strength of the colloid changes affecting the double-layer thickness and hence the final organization process. There must be a relationship between the deposition rate and the evaporation rate to structure of the particle coatings. Velev and coworkers[154] have observed the structural transitions in the thin films of latex particles and presented operational "phase" diagram, and obtained centimeter sized, homogeneous and well-ordered monolayer of latex spheres in controlled humidity. In our works, we also observed the formation of different structures in the coating of silica microspheres and succeed in obtaining large area uniform closely-packed monolayers of silica microspheres in the lab conditions.[155] It worthwhile note that we found that the solvent is one of the most critical factor to the formation of larger-area uniform closely-packed monolayers of particles. This suggests that the formation of uniform closely-packed monolayers of silica microparticles not only involves lateral capillary forces and convective flux, but also DLVO force and non-DLVO force and particle-substrate and particle–particle interactions.

Recently, the convective coating mechanism in the formation of micro- and nano-particles self-assembly structures have been revealed in many observations.[69, 95, 150–156] However, the parameters that govern the self-assembly process are not completely quantified, and still need to explore the complex interaction occurred in the convective coating process.

REVIEW

3.3.2. Application and Development

During the last few years, ordered arrays from various nano- and mcirosized particles were obtained by the convective coating or its modifications, such as ring formation in drying droplets.[165–168] to ordered deposits on the periphery of holes from dewetting films[169] to colloidal crystal formation in thin wetting films[150, 170, 171] and ultrathin mesoporous silica films.[172] Coatings of virtually any colloid and particles suspension can be easily deposited as long as the particles are entrained by the evaporation-driven flow. Several research groups suggested new versions of equipment or procedures, which were aimed at improving the control or at simplifying the procedures for particle array formation.

The convective coating process can be carried out by the relatively simple procedures, which drag upward an inclined glass plate immersed into the particles solution or dropped small volume solution on an inclined glass[173] Vengallatore and coworkers.[174] reported fabricating ordered arrays of colloidal micro- and nano-particles on the internal surfaces of geometrically complex, bulk-micromachined silicon structures. These structures could be applied to the incorporation of catalysts into microchemical reators and colloidal lithography on internal surfaces for controlling biocompatibility in microsystems used in biology and medicine. Colvin and coworkers[170] obtained large single-crystal colloidal multilayers of silica particles on substrates by means of vertical convective coating. These samples were planar to the substrate

by controlled evaporation of the disperse medium and the ensuring action capillary forces and make them ideally suited for optical characterization. However, this procedure is not efficient ways because coatings have to be done with large volume solution and vacuum oven and finished in several hours. Dimitrov and Nagayama[153] developed a setup which resembles in construction the dip-coating apparatus: by appropriate control of the rates of water evaporation and substrate withdrawal, they obtained centimeter sized, homogeneous in thickness, ordered arrays of latex particles.

Park and coworkers[175] presented confined convective assembly to produce well-ordered 2D and 3D polystyrene colloidal crystal films on over larger areas in several minute. The schematic experimental setup and illustration of colloidal particles assembly were depicted in Figure 19. Two glass substrates with a gap approximately 100 μm attached together. The PS colloidal suspension was dropped into the gap, and then dipped one glass substrate which controlled by dipping machine while blowing hot air towards the meniscus that formed at the interface of the glass substrate and the colloidal suspension, finally, the colloidal particles into ordered structure on the glass substrate. The advantage of this method is 2D and 3D colloidal crystals can be fabricated with a minute amount of PS colloidal suspension by controlled the lift-up rate which affects the meniscus-thinning rate. One interesting observation in their studies was binary colloidal crystals by consecutively depositing large and small particles were fabricated by this method.[175]

Ozin and Kitaev[176] also achieved the binary mixtures self-assembly structure consisted of large negatively charged polystyrene latex and much smaller negatively charged silica or PS latex spheres by accelerated evaporation of binary dispersions which is the key to ordering large latex spheres in the presence of smaller spheres. These structures can be used in microsphere template and for producing different types of clusters of monodispersed spheres without the need for photolithography.

Velev, Dimitrov and coworkers[96, 154–156, 177–187] have made significant advances in the development and application of the convective coating technology in past few years. They developed a convenient convective coating technique by dragging a liquid meniscus at constant velocity along a solid surface,[154] as show in Figure 18. The advantages of their technique are that the process of micro- and nanoparticles coating is simple, rapid, precise, controllable and depositing coatings save material by coating only a single surface of the substrate. They have succeeded in obtaining uniform centimeters coatings in minutes at rate approaching 100 μm/s from microliters of polystene spheres suspension.[154] They have fabricated a wide variety of different coatings including ferrin proteins,[182] nano-coatings from tobacco mosaic virus and silica nanoparticles,[154] latex crystals,[155, 178] inverse opal structure,[179, 181] and further applied to these structures in the fields of conductive

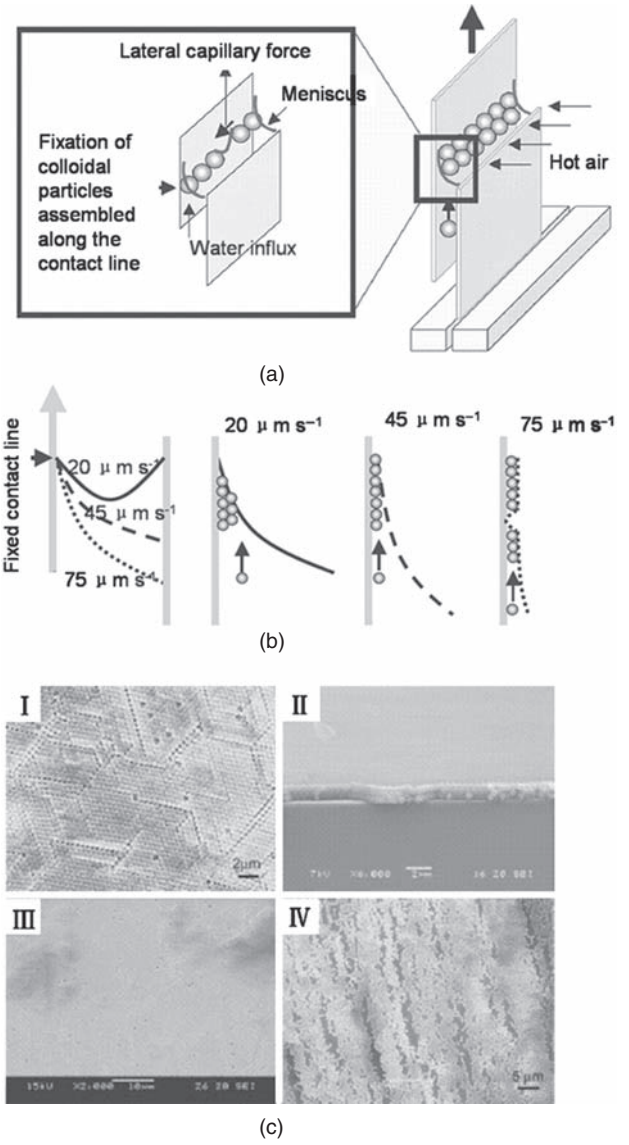

Fig. 19. (a) The experimental setup of confined convective assembly, (b) The shape of the meniscus as it varies with lift-up rate of 20 μms^{-1}, 45 μms^{-1}, and 75 μms^{-1}, (c) SEM images of polystyrene colloidal crystals with different lit-up rates of 20 μms^{-1}, 45 μms^{-1}, and 75 μms^{-1}. Reprinted with permission from [195], M. H. Kim et al., *Adv. Funct. Mater.* 15, 1329 **(2005)**. © 2005, Wiley-VCH.

and antirereflective coatings,[155] surface-enhancing Raman scattering substrates,[181] and lithographic masks[185] and so on. Following a similar idea, we recently, fabricated large-area uniform 2 μm silica microspheres monolayers with a high average surface coverage of over 85% on a 6×6 in^2 glass substrate which is the largest substrate we have attempted so far.[157] The loosely-packed submonolayers were observed on both of side of substrate due to the non-homogeneous particles in the suspension. This problem can be solved by continual supply of the suspension to the meniscus using a liquid injection system. This represents an effective and cheaper and controllable method

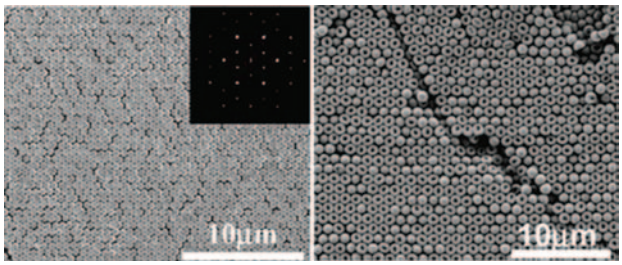

(a) (b)

Fig. 20. Hexagonally close-packed monolayers (a) and multilayers (b) of mushroom cap particles via convective assembly. Reprinted with permission from [190], I. D. Hosein and C. M. Liddell, *Langmuir* 23, 8810 **(2007)**. © 2007, American Chemical Society.

for the fabrication of particle monolayers with potentially industrial applications. Additionally, the uniform monolayer of silica microspheres further treated to form hemispheres surface textured structures as antireflective coating used on the amorphous silicon solar cells and organic solar cells.[157, 188]

Convective coating technique has been successfully applied to the self-assembly of non-spherical colloids.[189–191] The hexagonal zeolite plates were coated onto the flat substrates by convective coating. Orientational order with plates aligned paralleled to the substrate was achieved in monolayers, but positional order was limited to small regions because of the size and shape polydispersity of the zeolite particles. Hosten and Liddell[197] fabricated the 2D and 3D coating with high degree of positional and orientational order from mushroom-cap, pear and peanut shaped colloids via a heat assisted vertical convective coating. Long-range hexagonal close-packed ordered arrays were obtained from as a result of the monodispersity and compatibility of the particle shape, as shown in Figure 20.[190] The ordering was explained by thermodynamic consideration, such as free-energy minimization, the restriction of the particle orientational freedom at the suspension drying front. However, the orientational ordering must be operated in the sufficiently low particle concentration in order to reduce the physical particle-particle interactions. Nonspherical based colloidal arrays in both 2D and 3D could lead to advances in the nanofabricated of complex devices and in the production of microlens arrays.

Several studies[192–194] showed that the convective coating is operative even for particles, which are captured in free-standing films. Therefore, the solid or liquid substrates are not a necessary component of the assembly process. Following this approach Denkov and coworkers[193] developed a new procedure for the preparation of vitrified aqueous films, which contain mono- or multi-layers of particles, suitable for electron cryomicroscopy. The method was applied to nanometer seized latex particles and to monodispersed vesicles made of a lipid-protein mixture.

The main advantages of convective coating are its diversity of application and processing speed at which materials can be deposited.[158] However, the coatings fabricated by convective coating are not perfect colloid crystals due to the nature of the drying process, and usually easily form a polycrystalline film, and therefore unsuitable for sing crystal application such as large area photonic materials.[158] Additionally, there are two problems to be solved for the realization of a useful assembly technique, namely, both high productivity and ordering over a large area should be simultaneously satisfied. These questions maybe improved well by a continuous feed of liquid suspension to the moving meniscus. The convective coating technique is well suited to fabrication of large area coatings, which do not require defect-free, perfect microstructures such as antireflective coating for windows or solar cells or substrates for SERS sensors.[158]

A comparison of these three wet coating techniques for particle self-assembly is summarized in Table I.

Table I. Comparison of three wet coating processes for particle self-assembly.

Characteristics	Dip coating	Spin coating	Convective coating
Precursor	Not too sensitive to solution properties	Stringent solvent properties, good for Newtonian fluids	Not too sensitive to solution properties
Operation	Vertical or angle-dependent	Horizontal	Vertical, horizontal or angle-dependent
Operation	Automatic	Automatic	Automatic
Deposition rate	Controllable	Controllable	Controllable
Amount of solution	Large	Small	Small
Temperature	Controllable	Controllable	Controllable
Substrate size	Small to large	Small to medium	Medium to large
Substrate shape	Unlimited	Flat only, and good for circular	Flat
Coating coverage	Two side	One side	One side
Coating thickness	Controllable	Controllable	Controllable
Thickness uniformity	Fair to good	Fair to good	Good
Scale-up capability	Excellent	Fair	Good
Cost of setup	Low to moderate	Low to moderate	Moderate

4. CONCLUSIONS AND PERSPECTIVES

The emerging field of nanoscience and nanoengineering are leading to unprecedented understanding and control over the fundamental building blocks of all physical matter. Today, the significant progress of nanotechnology has been made by used in variety of fields. There is a need to learn how to manipulate micro- and nanosized particles to form the expected ordered structures for application into devices making use of the special properties. Particle self-assembly technology provides exceptional potentials to achieve 1D, 2D, and 3D structures for a wide variety of applications ranging from photonic devices to memory devices, single-electron microelectronic devices and so on. In order to make full use of the potentials for material engineering, it is important to identify and gain control over the assembly dynamic and the relevant ordering parameters both during the formation of ordered structures as well as after the growth process, so that the structures formed do not get distorted.

Particle self-assembly is a field in its nascent stage and experimentalists are still struggling to build up on the ideas propagated by the theorists to develop the complex technology required to construct 2D or 3D structures on the micro- or nanoscale. The understanding of the assembling dynamics helps us to control the forces guiding particle assembly that allows for constructing desired structures. Experimental research into localized vdW forces, electrostatic forces and other forces is underway. The study of these fundamental physical phenomena requires detailed analysis and experiments. The applications of the traditional dip coating and spin coating techniques and their modifications in particle self-assembly make simple, rapid, cheap and highly reproducible method to fabricate 2D or 3D particle arrays a possibility. The development of the convective coating technique is significant in the fabrication of the large area uniform well-ordered monolayers or multilayer of particles, with great potentials in industrial applications.

However, the relation between coating parameters and structural characteristics of assembled particle structures is not well understood. The development of a high-productivity wet-assembly method that can control the assembly structure and higher order structure has yet to be scaled up into practical technology. One of the main obstacles for putting into practice the interesting optical and structural properties of particle self-assembly structure in actual devices is the incompatibility of the time-consuming and unclean self-assembly crystallization techniques commonly used to make particle self-assembly with the fast and dirty-free technology required to fabricate devices. Most techniques developed to date are very sensitive to small variations of ambient humidity or temperature, which affect the lattice thickness and degree of crystalline. This makes it difficult to tailor the properties of the material. Non-spherical particles require tight control and alignment of their particle orientations during the assembling process in order to produce crystalline structures. It is evident that future advancements in particle self-assembly technology should greatly depend on new scientific breakthroughs, leading to the development of more efficient technologies for fabrication of hierarchical structures with well-defined dimensions, complexities and symmetries of morphologies, and chemical characters into order to realize designed functions.

Acknowledgments: The authors acknowledge financial support for this work from NSF under grants No. 0740147 and DMI-0625728, Texas Ignition Fund, and AFRL CONTACT Program under FA8650-07-2-5061.

References and Notes

1. J. M. Weissman, H. B. Sunkara, A. S. Tse et al., *Science* 274, 959 (**1996**).
2. E. A. Kamenetzky, L. G. Magliocco, and H. P. Panzer, *Science* 263, 207 (**1994**).
3. S. Sun, C. B. Murray, D. Weller et al., *Science* 287, 1989 (**2000**).
4. H. H. Pham, I. Gourevich, J. K. Oh et al., *J. Biomed. Mater. Res.* 59, 429 (**2002**).
5. I. Gourevich, H. H. Pham, J. K. Oh, J. E. N. Jonkman, E. Kumacheva, *Adv. Mat.* 16, 516 (**2004**).
6. J. H. Holtz and S. A. Asher, *Nature* 383, 829 (**1997**).
7. A. C. Sharma, T. Jana, R. Kesavamoorthy et al., *J. Am. Chem. Soc.* 126, 2971 (**2004**).
8. S. Kronholz, S. Rathgeber, S Karthäuser et al., *Adv. Funct. Mater.* 16, 2346 (**2006**).
9. A. K. Srivastava, S. Madhavi, T. J. White et al., *J. Mat. Chem.* 15, 4424 (**2005**).
10. A. N. Shipway, E. Katz, and I. Willner, *ChemPhysChem* 1, 18 (**2000**).
11. A. N. Shipway and I. Willner, *Chem. Commun.* 20, 2035 (**2001**).
12. S. A. Empedocles, R. Neuhauser, K. Shimizu et al., *Adv. Mater.* 11, 1243 (**1999**).
13. A. L. Efros and M. Rosen, *Annu. Rev. Mat. Sci.* 30, 475 (**2000**).
14. A. D. Yoffe, *Adv. Phys.* 51, 799 (**2002**).
15. S. A. Asher, Google Patents (**1986**).
16. M. Miyaki, K. Fujimoto, and H. Kawaguchi, *Col. Surf. A* 153, 603 (**1999**).
17. A. Taleb, V. Russier, A. Courty et al., *Phys. Rev. B* 59, 13350 (**1999**).
18. J. J. Shiang, J. R. Heath, C. P. Collier et al., *J. Phys. Chem. B* 102, 3425 (**1998**).
19. C. B. Murray, C. R. Kagan, and M. G. Bawendi, *Science* 270, 1335 (**1995**).
20. S. Maenosono, C. D. Dushkin, S. Saita et al., *Jpn. J. Appl. Phys. Part 1* 39, 4006 (**2000**).
21. S. Maenosono, E. Ozaki, K. Yoshie et al., *Jpn. J. Appl. Phys.* 40, 638 (**2001**).
22. A. V. Malko, A. A. Mikhailovsky, M. A. Petruska et al., *Appl. Phys. Lett.* 81, 1303 (**2002**).
23. S. Sun and C. B. Murray, *J. Appl. Phys.* 85, 4325 (**1999**).
24. N. Bowden, A. Terfort, J. Carbeck et al., *Science* 276, 233 (**1997**).
25. C. J. Brinker, *MRS Bull.* 29, 631 (**2004**).
26. M. Boncheva and G. M. Whitesides, *MRS Bull.* 30, 736 (**2005**).
27. G. M. Whitesides and B. Grzybowski, *Science* 295, 2418 (**2002**).
28. S. C. Glotzer, M. J. Solomon, and N. A. Kotov, *Am. Inst. Chem. Eng. J.* 50, 2978 (**2004**).

29. K. Hosokawa, I. Shimoyama, and H. Miura, *Sens. Actua.* 57, 117 **(1996)**.
30. K. E. Dungey, G. Lisensky, and S. M. Condren, *J. Chem. Ed.* 77, 618 **(2000)**.
31. T. Cui, F. Hua, and Y. Lvov, *Sens. Actuators, A* 114, 501 **(2004)**.
32. O. D. Velev, *Science* 312, 376 **(2006)**.
33. D. Chen, *Sol. Energ. Mater. Sol. Cells* 68, 313 **(2001)**.
34. P. A. Kralchevsky and N. D. Denkov, *Curr. Opin. Colloid Interface Sci.* 6, 383 **(2001)**.
35. D. Velegol, *J. Nanophoton.* 1, 012502 **(2007)**.
36. D. Wang and H. Möhwald, *J. Mat. Chem.* 14, 459 **(2004)**.
37. V. Shklover and H. Hofmann, edited by A. A. Balandin and K. L. Wang, American Scientific Publishers, Los Angeles **(2005)**, Vol. 2, p. 181.
38. S. Maenosono, T. Okubo, and Y. Yamaguchi, *J. Nanoparticle Res.* 5, 5 **(2003)**.
39. D. Grasso, K. Subramaniam, M. Butkus et al., *Rev. Environ. Sci. Biotechnol.* 1, 17 **(2002)**.
40. Q. Li, U. Jonas, X. S. Zhao et al., *Asia-Pac. J. Chem. Eng.* 3, 255 **(2008)**.
41. C. J. van Oss, R. F. Giese, and P. M. Costanzo, *Clays Clay Miner.* 38, 151 **(1990)**.
42. D. N. Petsev and P. G. Vekilov, *Phys. Rev. Lett.* 84, 1339 **(2000)**.
43. S. R. Raghavan, H. J. Walls, and S. A. Khan, *Langmuir* 16, 7920 **(2000)**.
44. G. Vigil, Z. Xu, S. Steinberg et al., *J. Colloid Interface Sci.* 165, 367 **(1994)**.
45. J. J. Adler, Y. I. Rabinovich, and B. M. Moudgil, *J. Colloid Interface Sci.* 237, 249 **(2001)**.
46. R. J. Hunter, Foundations of Colloid Science, Clarendon Press, **(1989)**.
47. A. Yethiraj and A. van Blaaderen, *Nature* 421, 513 **(2003)**.
48. J. N. Israelachvili, **(1992)**.
49. M. A. Bevan and D. C. Prieve, *Langmuir* 15, 7925 **(1999)**.
50. H. Y. Kim, J. O. Sofo, D. Velegol et al., *Langmuir* 23, 1735 **(2007)**.
51. H. Y. Kim, J. O. Sofo, D. Velegol et al., *J. Chem. Phys.* 124, 074504 **(2006)**.
52. J. Gregory, *J. Colloid Interface Sci.* 51, 44 **(1975)**.
53. M. Elimelech, Particle Deposition and Aggregation: Measurement, Modelling and Simulation, Butterworth-Heinemann **(1998)**.
54. M. Hu, S. Chujo, H. Nishikawa et al., *J. Nanoparticle Res.* 6, 479 **(2004)**.
55. E. Adachi and K. Nagayama, *Langmuir* 12, 1836 **(1996)**.
56. S. C. Rodner, P. Wedin, and L. Bergstrom, *Langmuir* 18, 9327 **(2002)**.
57. M. Retsch, Z. Zhou, S. Rivera et al., *Macromol. Chem. Phys.* 210, 230 **(2009)**.
58. T. Okubo, S. Chujo, S. Maenosono et al., *J. Nanoparticle Res.* 5, 111 **(2003)**.
59. B. Pansu, Pi. Pieranski, and Pa. Pieranski, *J. Physique* 45, 331 **(1984)**.
60. C. A. Murray and D. H. Van Winkle, *Phys. Rev. Lett.* 58, 1200 **(1987)**.
61. A. F. Routh and W. B. Russel, *AIChE J.* 44, 2088 **(1998)**.
62. R. Zangi and S. A. Rice, *Phys. Rev. E* 61, 660 **(2000)**.
63. M. Schmidt and H Löwen, *Phys. Rev. Lett.* 76, 4552 **(1996)**.
64. H. J. Butt, M. Kappl, H. Mueller et al., *Langmuir* 15, 2559 **(1999)**.
65. S. Block and C. A. Helm, *Phys. Rev. E* 76, 30801 **(2007)**.
66. J. L. Keddie, *Mater. Sci. Eng. R* 21, 101 **(1997)**.
67. D. Quemada and C. Berli, *Adv. Colloid Inter. Sci.* 98, 51 **(2002)**.
68. S. Hachisu and K. Takano, *Adv. Colloid Interface Sci.* 16, 233 **(1982)**.
69. N. D. Denkov, O. D. Velev, P. A. Kralchevsky et al., *Nature* 361, 26 **(1993)**.
70. J. Y. Walz and A. Sharma, *J. Colloid Interface Sci.* 168, 485 **(1994)**.
71. S. Asakura and F. Oosawa, *J. Chem. Phys.* 22, 1255 **(1954)**.
72. D. L. Sober and J. Y. Walz, *Langmuir* 11, 2352 **(1995)**.
73. R. Verma, J. C. Crocker, T. C. Lubensky et al., *Phys. Rev. Lett.* 81, 4004 **(1998)**.
74. A. Sharma, S. N. Tan, and J. Y. Walz, *J. Colloid Interface Sci.* 190, 392 **(1997)**.
75. S. Asakura and F. Oosawa, *J. Polym. Sci.* 33, 183 **(1958)**.
76. A. P. Chatterjee and K. S. Schweizer, *J. Chem. Phys.* 109, 10464 **(1998)**.
77. W. R. Bowen and P. M. Williams, *J. Colloid Interface Sci.* 184, 241 **(1996)**.
78. T. G. Mason, *Phys. Rev. E* 66, 60402 **(2002)**.
79. S. Badaire, C. Cottin-Bizonne, J. W. Woody et al., *J. Am. Chem. Soc.* 129, 40 **(2007)**.
80. K. Wostyn, Y. Zhao, B. Yee et al., *J. Chem. Phys.* 118, 10752 **(2003)**.
81. S. O. Lumsdon, E. W. Kaler, J. P. Williams et al., *Appl. Phys. Lett.* 82, 949 **(2003)**.
82. H. K. Christenson, P. M. Claesson, J. Berg et al., *J. Phys. Chem.* 93, 1472 **(1989)**.
83. H. K. Christenson, J. Fang, B. W. Ninham et al., *J. Phys. Chem.* 94, 8004 **(1990)**.
84. H. Onoe, K. Matsumoto, and I. Shimoyama, *Presented at the 17th International Conference on Micro Electro Mechanical Systems* (*MEMS*) **(2004)**, unpublished.
85. H. Onoe, K. Matsumoto, and I. Shimoyama, *J. Microelectron. Sys.* 13, 603 **(2004)**.
86. Z. Tang, Z. Zhang, Y. Wang et al., *Science* 314, 274 **(2006)**.
87. L. Pauling, The Nature of the Chemical Bonds, Cornell Univ. Press, NY **(1960)**, Vol. 224.
88. B. Pansu, P. Pieranski, and L. Strzelecki, *J. Physique* 44, 531 **(1983)**.
89. O. D. Velev, Handbook of Surfaces and Interfaces of Materials, Assembly of Colloidal Particles Into Nanostructured Materials and Microscopic Devices **(2001)**, Vol. 3.
90. P. A. Kralchevsky and K. Nagayama, *Langmuir* 10, 23 **(1994)**.
91. O. D. Velev, N. D. Denkov, V. N. Paunov et al., *Langmuir* 9, 3702 **(1993)**.
92. S. Maenosono, C. D. Dushkin, Y. Yamaguchi et al., *Colloid Polym. Sci.* 277, 1152 **(1999)**.
93. H. Nishikawa, S. Maenosono, Y. Yamaguchi et al., *J. Nanoparticle Res.* 5, 103 **(2003)**.
94. D. Gasperino, L. Meng, D. J. Norris et al., *J. Cryst. Growth* 310, 131 **(2008)**.
95. N. Denkov, O. Velev, P. Kralchevski et al., *Langmuir* 8, 3183 **(1992)**.
96. K. P. Velikov, F. Durst, and O. D. Velev, *Langmuir* 14, 1148 **(1998)**.
97. R. Aveyard, J. H. Clint, D. Nees et al., *Langmuir* 16, 1969 **(2000)**.
98. J. S. Smith, M. A. Hadley, G. S. Craig et al., Method and Apparatus for Fluid Self Assembly **(2003)**.
99. I. Soga, Y. Ohno, S. Kishimoto et al., *Jpn. J. Appl. Phys.* 42, 2226 **(2003)**.
100. L. E. Scriven, *MRS Mater. Res. Soc. Symp. Proc.* 121, 717 **(1988)**.
101. L. D. Landau and B. G. Levich, *Acta Physicochim. URSS* 17, 42 **(1942)**.
102. Y. Wang, H. Yang, L. Chen et al., *Presented at the 8th IEEE Conference on Nanotechnology* (*IEEE-NANO*), Arlington, TX **(2008)**, unpublished.
103. H. Ko, H. W. Lee, and J. Moon, *Thin Solid Films* 447, 638 **(2004)**.
104. C. Falamaki, M. Naimi, and A. Aghaie, *J. Eur. Ceram. Soc.* 26, 949 **(2006)**.
105. K. Kajihara, K. Nakanishi, K. Tanaka et al., *J. Am. Ceram. Soc.* 81, 2670 **(1998)**.
106. M. P. Tate, B. W. Eggiman, J. D. Kowalski et al., *Langmuir* 21, 10112 **(2005)**.
107. H. Kozuka, M. Kajimura, T. Hirano et al., *J. Sol–Gel Sci. Technol.* 19, 205 **(2000)**.

108. N. J. Arfsten, A. Eberle, J. Otto et al., *J. Sol–Gel Sci. Technol.* 8, 1099 (**1997**).
109. Y. Wang, L. Chen, H. Yang et al., Presented at the MRS Fall Meeting, Boston, MA (**2008**), unpublished.
110. D. Nagao, R. Kameyama, Y. Kobayashi et al., *Col. Surf. A* 311, 26 (**2007**).
111. D. Nagao, R. Kameyama, H. Matsumoto et al., *Col. Surf. A* 317, 722 (**2008**).
112. E. Bormashenko, R. Pogreb, O. Stanevsky et al., *Polym. Adv. Technol.* 16, 299 (**2005**).
113. J. Huang, R. Fan, S. Connor et al., *Angew. Chem. Int. Ed.* 46, 2414 (**2007**).
114. D. E. Bornside, C. W. Macosko, and L. E. Scriven, *J. Imag. Tech.* 13, 122 (**1987**).
115. S. Attia, J. Wang, G. Wu et al., *J. Mater. Sci. Technol.* 18, 211 (**2002**).
116. D. Meyerhofer, *J. Appl. Phys.* 49, 3993 (**1978**).
117. H. Kawakami, M. Mikawa, and S. Nagaoka, *J. Membr. Sci.* 137, 241 (**1997**).
118. D. Wang and H. Mohwald, *Adv. Mat.* 16, 244 (**2004**).
119. H. W. Deckman, J. H. Dunsmuir, S. Garoff et al., *J. Vac. Sci. Tech. B* 6, 333 (**1988**).
120. H. W. Deckman and J. H. Dunsmuir, *J. Vac. Sci. Tech. B* 1, 1109 (**1983**).
121. F.-K. Liu, Y.-C. Chang, F.-H. Ko et al., *Microelectron. Eng.* 67–68, 702 (**2003**).
122. H. W. Deckman and J. H. Dunsmuir, *Appl. Phys. Lett.* 41, 377 (**1982**).
123. D. Y. Godovsky, *Adv. Polym. Sci.* 153, 163 (**2000**).
124. H. Dollefeld, H. Weller, and A. Eychmuller, *J. Phys. Chem. B* 106, 5604 (**2002**).
125. Y. K. Hong, H. Kim, G. Lee et al., *Appl. Phys. Lett.* 80, 844 (**2002**).
126. M. Tao, W. Zhou, H. Yang et al., *Appl. Phys. Lett.* 91, 081118 (**2007**).
127. Y. Xu, G. J. Schneider, E. D. Wetzel et al., *Presented at the Proc. of SPIE* (**2003**), unpublished.
128. T. Ogi, L. B. Modesto-Lopez, F. Iskandar et al., *Col. Surf. A* 297, 71 (**2007**).
129. J. C. Hulteen and R. P. V. Duyne, *J. Vac. Sci. Tech. A* 13, 1553 (**1995**).
130. G. A. Ozin and S. M. Yang, *Adv. Funct. Mater.* 11, 95 (**2001**).
131. D. Xia and S. R. J. Brueck, *Nano Lett.* 4, 1295 (**2004**).
132. P. Jiang and M. J. McFarland, *J. Am. Chem. Soc.* 126, 13778 (**2004**).
133. P. Jiang, T. Prasad, M. J. McFarland et al., *Appl. Phys. Lett.* 89, 011908 (**2006**).
134. W. L. Min, P. Jiang, and B. Jiang, *Nanotechnology* 19, 475604 (**2008**).
135. C. H. Sun, B. J. Ho, B. Jiang et al., *Opt. Lett.* 33, 2224 (**2008**).
136. B. J. Ackerson, *J. Rheol.* 34, 553 (**1990**).
137. B. J. Ackerson and P. N. Pusey, *Phys. Rev. Lett.* 61, 1033 (**1988**).
138. R. M. Amos, T. J. Shepherd, J. G. Rarity et al., *Electron. Lett.* 36, 1411 (**2000**).
139. L. B. Chen, B. J. Ackerson, and C. F. Zukoski, *J. Rheol.* 38, 193 (**1994**).
140. R. L. Hoffman, *J. Rheol.* 16, 155 (**1972**).
141. P. Pieranski, *Cont. Phys.* 24, 25 (**1983**).
142. J. Vermant and M. J. Solomon, *J. Phys.: Condens. Matter* 17, R187 (**2005**).
143. C. H. Sun, W. L. Min, and P. Jiang, *Chem. Commun.* 2008, 3163 (**2008**).
144. P. Jiang and M. J. McFarland, *J. Am. Chem. Soc.* 127, 3710 (**2005**).
145. P. Jiang, *Langmuir* 22, 3955 (**2006**).
146. C. H. Sun, P. Jiang, and B. Jiang, *Appl. Phys. Lett.* 92, 061112 (**2008**).
147. W. L. Min, B. Jiang, and P. Jiang, *Adv. Mat.* 20, 3914 (**2008**).
148. C. H. Sun, W. L. Min, N. C. Linn et al., *Appl. Phys. Lett.* 91, 231105 (**2007**).
149. A. Mihi, M. Ocana, and H. Miguez, *Adv. Mater.* 18, 2244 (**2006**).
150. C. D. Dushkin, H. Yoshimura, and K. Nagayama, *Chem. Phys. Lett.* 204, 455 (**1993**).
151. C. D. Dushkin, G. S. Lazarov, S. N. Kotsev et al., *Colloid Polym. Sci.* 277, 914 (**1999**).
152. A. S. Dimitrov and K. Nagayama, *Chem. Phys. Lett.* 243, 462 (**1995**).
153. A. S. Dimitrov and K. Nagayama, *Langmuir* 12, 1303 (**1996**).
154. B. G. Prevo and O. D. Velev, *Langmuir* 20, 2099 (**2004**).
155. B. G. Prevo, Y. Hwang, and O. D. Velev, *Chem. Mater.* 17, 3642 (**2005**).
156. B. G. Prevo, E. W. Hon, and O. D. Velev, *J. Mat. Chem.* 17, 791 (**2007**).
157. Y. Wang, L. Chen, H. Yang et al., *Solar Energy Materials and Solar Cells* 93, 85 (**2009**).
158. B. G. Prevo, D. M. Kuncicky, and O. D. Velev, *Col. Surf. A* 311, 2 (**2007**).
159. C. A. Fustin, G. Glasser, H. W. Spiess et al., *Langmuir* 20, 9114 (**2004**).
160. L. Shmuylovich, A. Q. Shen, and H. A. Stone, *Langmuir* 18, 3441 (**2002**).
161. K. Lin, J. C. Crocker, V. Prasad et al., *Phys. Rev. Lett.* 85, 1770 (**2000**).
162. M. Heni and H. Lowen, *Phys. Rev. Lett.* 85, 3668 (**2000**).
163. P. V. Braun, R. W. Zehner, C. A. White et al., *Adv. Mater.* 13, 721 (**2001**).
164. J. W. G. Tyrrell and P. Attard, *Colloids Surf. A Phys. Rev. Lett.* 87, 176104 (**1997**).
165. R. D. Deegan, O. Bakajin, T. F. Dupont et al., *Nature* 389, 827 (**1997**).
166. R. D. Deegan, O. Bakajin, T. F. Dupont et al., *Phys. Rev. E* 62, 756 (**2000**).
167. E. Adachi, A. S. Dimitrov, and K. Nagayama, *Langmuir* 11, 1057 (**1995**).
168. V. X. Nguyen and K. J. Stebe, *Phys. Rev. Lett.* 88, 164501 (**2002**).
169. P. C. Ohara and W. M. Gelbart, *Langmuir* 14, 3418 (**1998**).
170. P. Jiang, J. F. Bertone, K. S. Hwang et al., *Chem. Mat.* 11, 2132 (**1999**).
171. Z. Z. Gu, A. Fujishima, and O. Sato, *Chem. Mater.* 14, 760 (**2002**).
172. Z. Yuan, D. B. Burckel, P. Atanassov et al., *J. Mater. Chem.* 16, 4637 (**2006**).
173. R. Micheletto, H. Fukuda, and M. Ohtsu, *Langmuir* 11, 3333 (**1995**).
174. S. Vengallatore, Y. Peles, L. R. Arana et al., *Sens. Actuators, A* 113, 124 (**2004**).
175. M. H. Kim, S. H. Im, and O. O. Park, *Adv. Mater.* 17, 2501 (**2005**).
176. V. Kitaev and G. A. Ozin, *Adv. Mater.* 15 (**2003**).
177. B. G. Prevo, Y. Hwang, and O. D. Velev, *Chem. Mater.* 17, 3642 (**2005**).
178. B. G. Prevo, J. C. Fuller III, and O. D. Velev, *Appl. Opt.* 37, 8030 (**1998**).
179. P. M. Tessier, O. D. Velev, A. T. Kalambur et al., *J. Am. Chem. Soc.* 122, 9554 (**2000**).
180. P. M. Tessier, S. D. Christesen, K. K. Ong et al., *Appl. Spectrosc.* 56, 1524 (**2002**).
181. D. M. Kuncicky, S. D. Christesen, and O. D. Velev, *Appl. Spectrosc.* 59, 401 (**2005**).
182. D. M. Kuncicky, K. Bose, K. D. Costa et al., *Chem. Mater.* 19, 141 (**2007**).
183. D. M. Kuncicky, S. D. Christesen, and O. D. Velev, *Proc. SPIE* 33 (**2004**).
184. D. M. Kuncicky, B. G. Prevo, and O. D. Velev, *J. Mat. Chem.* 16, 1207 (**2006**).

185. N. H. Finkel, B. G. Prevo, O. D. Velev et al., *Anal. Chem.* 77, 1088 (**2005**).
186. D. M. Kuncicky, K. Bose, K. D. Costa et al., *Nature* 389, 827 (**1997**).
187. V. Rastogi and O. D. Velev, *Biomicrofluidics* 1, 014107 (**2007**).
188. Y. Wang, R. Tummala, L. Chen et al., *J. Appl. Phys.* (**2009**), in press.
189. J. A. Lee, L. Meng, D. J. Norris et al., *Langmuir* 22, 5217 (**2006**).
190. I. D. Hosein and C. M. Liddell, *Langmuir* 23, 8810 (**2007**).
191. I. D. Hosein and C. M. Liddell, *Langmuir* 23, 10479 (**2007**).
192. N. D. Denkov, H. Yoshimura, K. Nagayama et al., *Phys. Rev. Lett.* 76, 2354 (**1976**).
193. N. D. Denkov, H. Yoshimura, and K. Nagayama, *Ultramicroscopy* 65, 147 (**1996**).
194. N. D. Denkov, H. Yoshimura, T. Kouyama et al., *Biophys. J.* 74, 1409 (**1998**).
195. M. H. Kim, S. H. Im, and O. O. Park, *Adv. Funct. Mater.* 15, 1329 (**2005**).

Received: 18 February 2009. Accepted: 19 April 2009.